Plant Physiology®

Plant Physiology, 2024, 00, 1–16
https://doi.org/10.1093/plphys/kiae292
Advance access publication 22 May 2024
Research Report

# Pinpointing the causal influences of stomatal anatomy and behavior on minimum, operational, and maximum leaf surface conductance

Marissa E. Ochoa,[1] Christian Henry,[1] Grace P. John,[2] Camila D. Medeiros,[1] Ruihua Pan,[3] Christine Scoffoni,[4] Thomas N. Buckley,[5] and Lawren Sack[1,*]

[1]Department of Ecology and Evolutionary Biology, University of California, Los Angeles, CA 90095, USA
[2]Department of Biology, University of Florida, Gainesville, FL 32611, USA
[3]School of Ecology and Environment, Inner Mongolia University, Hohhot, 010021, China
[4]Department of Biological Sciences, California State University, Los Angeles, CA 90032, USA
[5]Department of Plant Sciences, University of California, Davis, CA 95616, USA
*Author for correspondence: lawrensack@ucla.edu
The author responsible for distribution of materials integral to the findings presented in this article in accordance with the policy described in the Instructions for Authors (https://academic.oup.com/plphys/pages/General-Instructions) is Lawren Sack.

## Abstract

Leaf surface conductance to water vapor and $CO_2$ across the epidermis ($g_{leaf}$) strongly determines the rates of gas exchange. Thus, clarifying the drivers of $g_{leaf}$ has important implications for resolving the mechanisms of photosynthetic productivity and leaf and plant responses and tolerance to drought. It is well recognized that $g_{leaf}$ is a function of the conductances of the stomata ($g_s$) and of the epidermis + cuticle ($g_{ec}$). Yet, controversies have arisen around the relative roles of stomatal density ($d$) and size ($s$), fractional stomatal opening ($\alpha$; aperture relative to maximum), and $g_{ec}$ in determining $g_{leaf}$. Resolving the importance of these drivers is critical across the range of leaf surface conductances, from strong stomatal closure under drought ($g_{leaf,min}$), to typical opening for photosynthesis ($g_{leaf,op}$), to maximum achievable opening ($g_{leaf,max}$). We derived equations and analyzed a compiled database of published and measured data for approximately 200 species and genotypes. On average, within and across species, higher $g_{leaf,min}$ was determined 10 times more strongly by $\alpha$ and $g_{ec}$ than by $d$ and negligibly by $s$; higher $g_{leaf,op}$ was determined approximately equally by $\alpha$ (47%) and by stomatal anatomy (45% by $d$ and 8% by $s$), and negligibly by $g_{ec}$; and higher $g_{leaf,max}$ was determined entirely by $d$. These findings clarify how diversity in stomatal functioning arises from multiple structural and physiological causes with importance shifting with context. The rising importance of $d$ relative to $\alpha$, from $g_{leaf,min}$ to $g_{leaf,op}$, enables even species with low $g_{leaf,min}$, which can retain leaves through drought, to possess high $d$ and thereby achieve rapid gas exchange in periods of high water availability.

## Introduction

The stomatal opening drives leaf surface conductance of water vapor from leaf to air ($g_{leaf-air}$; symbols and units are defined in Table 1) and regulates transpiratory water loss at a given leaf to air vapor pressure difference and boundary layer conductance. A high $g_{leaf-air}$ also represents high conductance to $CO_2$, which strongly contributes to higher photosynthetic rates, and scales up, in combination with leaf area allocation, to a greater ecosystem net primary productivity (Wang et al. 2015). $g_{leaf-air}$ is determined by the conductance of vapor to pathways across the leaf surface ($g_{leaf}$), in series with the boundary layer ($g_{bl}$), with $g_{leaf}$ being the dominant influence at moderate to high wind speeds when $g_{bl}$ is large (Fig. 1). In turn, $g_{leaf}$ is determined by the parallel conductances of the stomata ($g_s$) and of leaf surfaces other than open stomatal pores (pathways across the epidermal cell walls and cuticle; $g_{ec}$) (Kerstiens 1996; Fernández and Eichert 2009). $g_s$ increases when stomata open in response to high irradiance and high-water status, resulting in an operational leaf surface conductance ($g_{leaf,op}$). Under certain conditions, including acclimation to low $CO_2$, stomatal conductance may increase to approach its anatomical maximum ($g_{leaf,max}$; Dow et al. 2014). By contrast, under the reverse conditions, stomatal closure results in a decline in $g_s$, caused by the loss of turgor pressure and shrinkage of guard cells driven by efflux of osmolytes, which, in the case of responses to water status, is associated with ABA signaling from tissues within the leaf (Xie et al. 2006; Bauer et al. 2013; McAdam and Brodribb 2015; Engineer et al. 2016). For most plants, substantial stomatal closure occurs at or before wilting, and $g_{leaf}$ declines to a minimum value, known as the "minimum leaf surface conductance" ($g_{leaf,min}$). Recent work on species around the world has clarified the importance of $g_{leaf,min}$ as a key contributor to drought tolerance (Kerstiens 1996; Martin-StPaul et al. 2017; Blackman et al. 2019; Duursma et al. 2019). Across species, a lower $g_{leaf,min}$ enables leaves to remain above lethal thresholds for dehydration longer for a given level of atmospheric drought caused by vapor pressure deficit (VPD), wind, and irradiance; thus, a lower $g_{leaf,min}$ contributes to leaf and plant survival from drought (Sack et al. 2003a; Sack and Tyree 2005; John et al. 2018; Blackman et al. 2019; López et al. 2021).

However, the relative roles of stomatal anatomy and behavior in defining variation within and across species in $g_{leaf}$ have remained controversial and unresolved in the literature, due to a

Received September 12, 2023. Accepted April 23, 2024.

**Table 1.** Symbols and definitions of stomatal traits and biophysical constants. This study required a more explicit and comprehensive definition of terms and symbols than typical in the previous literature on stomatal traits, i.e. distinguishing leaf–air surface conductance ($g_{leaf–air}$) from leaf surface conductance ($g_{leaf}$) and from stomatal conductance ($g_s$), with subscripts indicating whether stomata are on average at minimum, operational, or maximum aperture. Our analyses focused on variables from published and novel measurements (m) or inferred based on relationships of traits in the published literature (i; estimating $g_{ec}$ from its relationship with $g_{leaf,min}$ in Machado et al. 2021 or sampling from the compiled diverse data of Kerstiens 1996) or derived (d). Diffusional conductances reported on a leaf area basis represent diffusion from both surfaces but are all normalized by the area of one side of the leaf

| Stomatal trait | Symbol | Units | Data source for analyses |
|---|---|---|---|
| *Diffusional conductances on a leaf area basis* | | All in mol $m^{-2}$ $s^{-1}$ | |
| Leaf to air | $g_{leaf,leaf–air}$ | | NA |
| Leaf boundary layer | $g_{bl}$ | | NA |
| Leaf when stomata fully closed | $g_{leaf,min}$ | | m |
| Leaf operational in conducting gas exchange | $g_{leaf,op}$ | | m |
| Leaf when stomata fully open | $g_{leaf,max}$ | | d |
| Stomata when fully open | $g_{s,max}$ | | d |
| Stomata while leaf operational in conducting gas exchange | $g_{s,op}$ | | d |
| Stomata when fully closed | $g_{s,min}$ | | d |
| Nonstomatal conductance ($g_{leaf} - g_s$) | $g_{ns}$ | | d |
| *Conductivities* | | All in mol $m^{-2}$ $s^{-1}$ | |
| Conductivity of open pore area | $g_p$ | | d |
| Conductivity of guard cell surface | $g_g$ | | d |
| Conductivity of epidermal cell surface | $g_e$ | | d |
| Conductivity of cutinized leaf epidermal surface | $g_{ec}$ | | i |
| *Tissue areas per stoma* | | All in $m^2$ $stoma^{-1}$ | |
| Area of stomatal pore (pore area per stoma) | $A_p$ | | d |
| Epidermal cell surface area per epidermal cell | $A_e$ | | d |
| Guard cell surface area per stoma | $A_g$ | | d |
| *Leaf-scale stomatal parameters* | | | |
| Stomatal density | $d$ | Stomata $m^{-2}$ | m |
| Stomatal size | $s$ | $m^2$ | m |
| Fraction of leaf area taken up by stomata | $f$ | Unitless | d |
| *Stomatal dimensions* | | All in m | |
| Length of stoma (= length of guard cell) | $L$ | | d |
| Width of stoma (= width of guard cell pair) | W | | d |
| *Pore dimensions* | | All in m | |
| Depth of stomatal pore | $l$ | | d |
| Length of stomatal pore | $p$ | | d |
| Aperture of stomatal pore | $a$ | | d |
| *Dimensionless scaling factors* | | All unitless | |
| Ratio of pore depth to pore length ($l/p$) | $j$ | | Constant |
| Ratio of pore length to stomatal length ($p/L$) | $c$ | | Constant |
| Ratio of $c$ to the square root of $j$ | $\mu$ | | Constant |
| Fractional stomatal opening (aperture relative to maximum) | $\alpha$ | | d |
| *Physical parameters* | | | |
| Binary diffusivity for water vapor in air | $D_{wa}$ | $m^2$ $s^{-1}$ | Constant |
| Molar volume of air | $V_{ma}$ | $m^3$ $mol^{-1}$ | Constant |
| Mean free path | x’ | m | Constant |

lack of unified concepts and data. There has not been a comprehensive analysis of the general determination of $g_{leaf}$ across the range of leaf water status, from $g_{leaf,min}$ to $g_{leaf,op}$ to $g_{leaf,max}$; thus, only correlative evidence has been available to test hypotheses for how these conductance variables depend on their underlying drivers. Here, we developed a theory to enable the quantification of the influence of traits on $g_{leaf}$ and assembled published data from studies of $g_{leaf}$, stomatal anatomy, and behavior across species for insights into the causal drivers of $g_{leaf}$ across its range. We designed our analyses to reconcile apparent conflicts in the literature by partitioning the importance of factors driving higher $g_{leaf}$ across its range, including stomatal anatomy (density, $d$; size, $s$), behavior during dehydration (fractional stomatal opening, i.e., aperture relative to maximum, $\alpha$), and $g_{ec}$.

The role of the stomatal anatomy in the determination of $g_{leaf,min}$ within and across species has been the subject of both longstanding and recent controversies (Kerstiens 1996; Machado et al. 2021; Slot et al. 2021). A well-known, pioneering study argued that stomatal density ($d$) strongly determined $g_{leaf,min}$ variation across 10 genotypes of *Sorghum bicolor* (sorghum) based on their strong correlation and inferred that stomatal anatomy was even more important than high $g_{ec}$ as a dominant cause of high $g_{leaf,min}$ in dehydrating leaves, with residual “stomatal leakiness” determining high $g_{leaf,min}$ (Muchow and Sinclair 1989). Yet, $g_{leaf,min}$ was independent of $d$ across individuals of 2 desert grass species (Smith et al. 2006) and across sun and shade leaves of 6 woody temperate species (Sack et al. 2003b). Across 30 Brazilian tree species, $g_{leaf,min}$ was correlated with $d$, suggesting that $d$ was an important driver of $g_{leaf,min}$ (Machado et al. 2021). The latter study further asserted that a high $d$ would be a general cause of both high $g_{leaf,max}$ and high $g_{leaf,min}$, resulting in a trade-off between maximum function and drought tolerance as, for species prone to drought, a low $g_{leaf,min}$, by necessitating a low $g_{leaf,max}$, would incur a cost to maximum photosynthetic rate and result in lower productivity when soil is moist (Machado et al. 2021). However, contrasting results were reported for cherry laurel (*Prunus laurocerasus*) (Diarte et al. 2021) and for 4 Panamanian woody angiosperm species (Slot et al. 2021). In these studies, aluminum tape was used to seal the abaxial (stomatal) surface, restricting diffusion solely to the nonstomatal adaxial side. Correcting for the exposed leaf area, those authors reported that $g_{leaf,min}$ did not change, thereby suggesting that the abaxial stomata had been completely sealed and did not

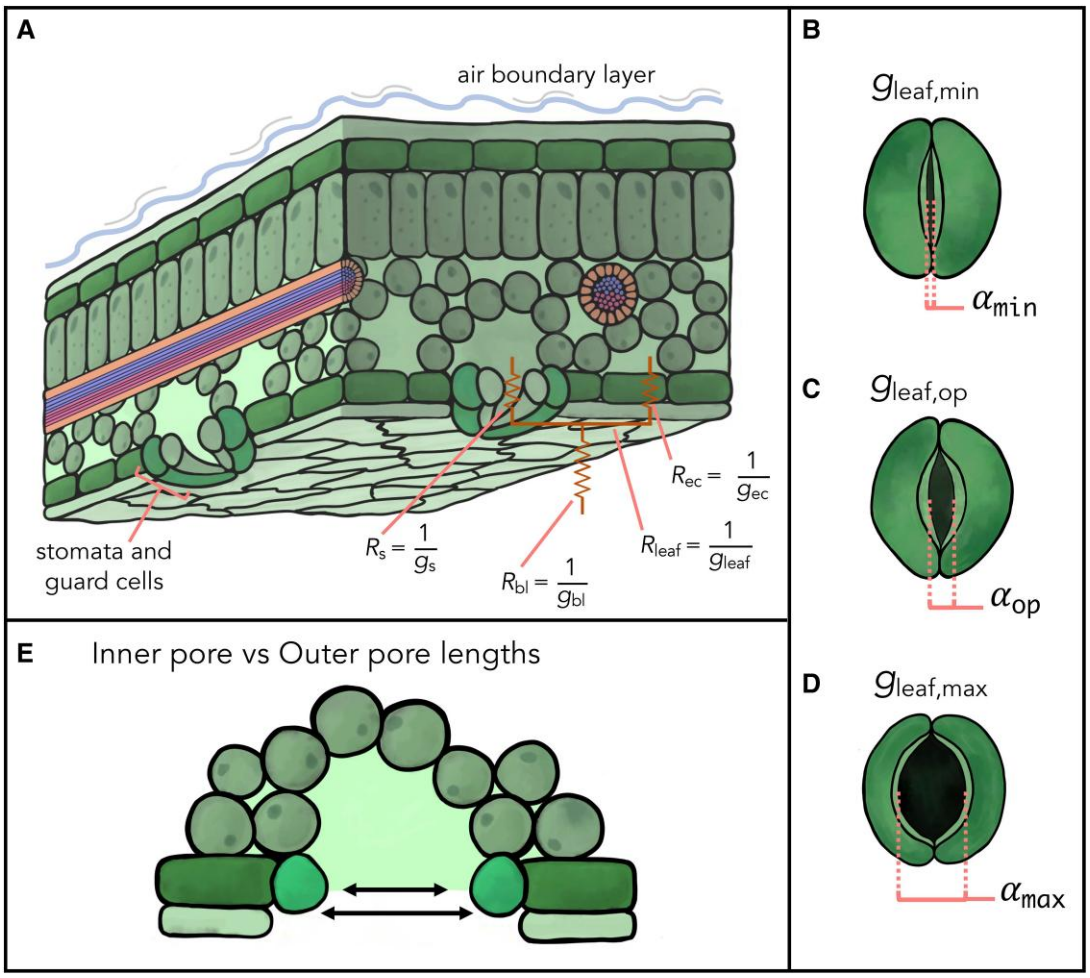


**Figure 1.** Determinants of leaf to air conductance ($g_{leaf–air}$). **A**) $g_{leaf–air}$ is determined by the leaf surface conductance ($g_{leaf}$) and the boundary layer conductance ($g_{bl}$). $g_{leaf}$, in turn, is a function of the stomatal conductance ($g_s$) and nonstomatal conductance across the epidermis and cuticle ($g_{ec}$), with $g_s$ as a function of stomatal density, size, and fractional aperture determined by the opening of guard cells, which surround the stomatal pore and depicted in **B**, **C**, and **D**, respectively, for stomata closed to their minimum for dehydrated leaves ($g_{leaf,min}$), open for operation under high irradiance diurnally ($g_{leaf,op}$), or open maximally ($g_{leaf,max}$). **E**) Guard cell pore flares away from the inner pore; thus, the inner pore can be narrower than the outer pore, which is visible in the top view, and the estimated apertures from the top-view stomata micrograph images can underestimate the apertures. Images partially inspired by Roussin-Léveillée et al. 2022 and in part created using BioRender.com.

influence the measured $g_{leaf,min}$. However, our reanalyses for the 4 Panamanian woody angiosperm species reveal substantial stomatal "leakiness" for 3/4 species, under moderate air temperatures (25 to 32 °C) (Supplementary Method S1; Supplementary Table S1). It is thus clear that in many species, the stomata are not completely closed in strongly dehydrated leaves and that causal rather than correlative analyses are needed to disentangle the roles of $d$, $s$, $\alpha$, and $g_{ec}$ in determining $g_{leaf,min}$.

The relative influences of stomatal anatomy and behavior on $g_{leaf,op}$ have also remained ambiguous. Several studies within and across diverse species found correlations of $g_{leaf,op}$ with the conductance of fully open stomata ($g_{s,max}$), which was calculated directly from measurements of $d$ and $s$, implying that anatomy is the major determinant of variation across leaves in $g_{leaf,op}$ (Drake et al. 2013; Dow et al. 2014; McElwain et al. 2016; Wu et al. 2020). In contrast, little is known of the importance of $\alpha$ and of $g_{ec}$ in determining variations within and across species in $g_{leaf,op}$, although some studies considered these as potentially key drivers (McElwain et al. 2016; Márquez et al. 2021, 2022; Cernusak and De Kauwe 2022).

Finally, while the determinants of $g_{leaf,max}$ have been described, assuming stomata to be open to the conventionally defined "maximum aperture" (in which the pore is circular), the importance of the given stomatal traits for explaining variations in $g_{leaf,max}$ has not been resolved. Many studies have attributed higher $g_{leaf,max}$ within and across species to greater densities of smaller stomata, given that these would increase the total pore area and reduce the pore depth for diffusion (Brown and Escombe 1900; Franks et al. 1998; Franks and Beerling 2009; Sack and Buckley 2016); however, the relative causal importance of variation in $d$ and $s$ in explaining variation in $g_{leaf,max}$ has not been quantified.

The disentangling of factors determining $g_{leaf}$ across its range can provide key insights into the mechanisms of drought tolerance and may also highlight targets for breeding for improved stress resilience and productivity. We developed a causal approach for this analysis because correlation analyses cannot accurately partition the relative mechanistic contributions of underlying factors to higher-level variables, such as $g_{leaf}$, given the covariation among variables (John et al. 2018). Thus, we derived equations for the biophysical determinants of $g_{leaf}$ from minimum stomatal opening, to operationally open stomata, and to full opening, thereby pinpointing the causal influences on $g_{leaf}$ of $d$, $s$, $\alpha$, and $g_{ec}$ in any scenario. We hypothesized that the influences of stomatal anatomy ($d$ and $s$) on $g_{leaf}$ across species would

be low for $g_{leaf,min}$, given stomatal closure, with fractional stomatal opening ($\alpha$) and $g_{ec}$ dominating, and the relative influence of $d$ and $s$ would increase for $g_{leaf,op}$ and $g_{leaf,max}$. We tested these hypotheses in a database of leaf surface conductance and stomatal anatomy for 203 diverse plant species and genotypes compiled from measured and published data (Supplementary Tables S2 and S3). As previous studies found that life form groups with different leaf ecologies potentially differed in the drivers of leaf surface conductances, i.e., woody deciduous vs. evergreen, vs. herbaceous/crop (Machado et al. 2021; Liu et al. 2023), we conducted analyses both within and across life form groups. We hypothesized that among deciduous woody species or herbaceous/crop species, $g_{leaf,min}$ and $g_{leaf,max}$ may be linked if certain species are selected for rapid growth and leaf turnover, although such a nonmechanistic linkage would not be general, as it could be broken due to variation in stomatal anatomy and behavior and $g_{ec}$.

# Results

## Equations for $g_{leaf}$ as a function of its determinants

We derived a general equation for $g_{leaf}$ as a function of $d$, $s$, $\alpha$, and $g_{ec}$, with extensions to the specific cases in which stomata are closed to their minimum ($g_{leaf,min}$), open operationally ($g_{leaf,op}$), or open to their maximum ($g_{leaf,max}$) (see Supplementary Method S2 for derivations). In these derivations, we excluded additional second-order factors that would reduce $g_{leaf}$, including (1) deviations of the stomatal pore from simplified cylindrical geometry (Franks and Farquhar 2007); (2) contribution of diffusion resistances in the intercellular airspaces, especially in the case of a partly cutinized substomatal chamber (Roth-Nebelsick 2007; Feild et al. 2011); (3) leaf surface features, such as trichomes or papillae surrounding the stomata, or encryption of stomata, which can affect diffusion through stomata and/or the boundary layer (Kenzo et al. 2008; Hassiotou et al. 2009; Maricle et al. 2009); and (4) stomatal clustering (Lehmann and Or 2015).

$$\begin{aligned} g_{leaf} &= \frac{D_{wa}\pi\alpha^2\mu^2 d_U s}{V_{ma}(4j+\pi\sqrt{\alpha})(x'+\alpha\mu\sqrt{s})} + \frac{D_{wa}\pi\alpha^2\mu^2 d_L s}{V_{ma}(4j+\pi\sqrt{\alpha})(x'+\alpha\mu\sqrt{s})} \\ &\quad + \left(1-\frac{\pi}{4}\alpha\mu^2 d_U s\right)g_{ec} + \left(1-\frac{\pi}{4}\alpha\mu^2 d_L s\right)g_{ec} \\ &= \frac{D_{wa}\pi\alpha^2\mu^2 d_T s}{V_{ma}(4j+\pi\sqrt{\alpha})(x'+\alpha\mu\sqrt{s})} + \left(2-\frac{\pi}{4}\alpha\mu^2 d_T s\right)g_{ec} \\ &= g_s + g_{ns}, \quad \text{where } g_s \equiv \frac{D_{wa}\pi\alpha^2\mu^2 d_T s}{V_{ma}(4j+\pi\sqrt{\alpha})(x'+\alpha\mu\sqrt{s})} \\ &\quad \text{and } g_{ns} \equiv \left(2-\frac{\pi}{4}\alpha\mu^2 d_T s\right)g_{ec} \end{aligned} \quad (1)$$

where $d_U$ and $d_L$ are stomatal densities (pores $m^{-2}$) on the adaxial and abaxial surfaces, respectively; $x''$ is the mean free path in air (the mean distance a gas molecule travels before colliding with another) (m); $g_{ec}$ is the conductance of the nonstomatal leaf surface area, i.e., of the epidermis and cuticle (mol $m^{-2}$ $s^{-1}$); $D_{wa}$ is the binary diffusivity of water vapor in air ($m^2$ $s^{-1}$); $V_{ma}$ is the molar volume of air ($m^3$ $mol^{-1}$); $\mu$ and $j$ are the dimensionless scaling factors that equal $1/\sqrt{2}$ and 0.5 for nongrasses and $\sqrt{2}$ and 0.125 for grasses (reflecting the distinct shape of stomata in grasses); and $g_{ns}$ is the conductance across all leaf surfaces other than open stomatal pores (i.e. $g_{ns} \equiv g_{leaf} - g_s$). We note that both $g_{ns}$ and $g_{ec}$ refer to the conductance of the epidermal cells + cuticle (i.e. the nonstomatal conductance) but are normalized differently. Thus, $g_{ec}$ refers to the conductance across the epidermal cell + cuticle per unit of nonstomatal area, while $g_{ns}$ refers to the conductance of epidermal cell + cuticle of both leaf surfaces expressed per unit of the one-sided leaf area. Given that $g_{ns}$ represents both leaf surfaces but is expressed on a one-sided leaf area basis, it tends to be almost double $g_{ec}$. Further, all else equal, $g_{ns}$ is higher when the open stomatal pore area is smaller, that is, for species with lower $d$ or $s$, and when the stomata close. Preserving the conventional, simple, and operational definition of $g_{ec}$ (an input into our equations), yet presenting our equations to express the roles of stomatal and nonstomatal conductances, required us to distinguish these two terms.

$g_{leaf,min}$, $g_{leaf,op}$, and $g_{leaf,max}$ are found by applying $\alpha_{min} = a_{min}/p$, $\alpha_{op} = a_{op}/p$, and $\alpha_{max} = a_{max}/p = 1$, respectively, to Equation (1), where $a_{min}$ and $a_{op}$ are stomatal apertures (m) and $p$ (m) is the stomatal pore length. This derivation follows theoretical assumptions (Franks and Beerling 2009; Sack and Buckley 2016) with empirical support (Dow et al. 2014) that the theoretical maximum anatomical opening is a circular pore, i.e., the maximum aperture width equals the pore length:

$$\begin{aligned} g_{leaf,\,min} &= \frac{D_{wa}\pi\alpha_{min}^2\mu^2 d_T s}{V_{ma}(4j+\pi\sqrt{\alpha_{min}})(x'+\alpha_{min}\mu\sqrt{s})} \\ &\quad + \left(2-\frac{\pi}{4}\alpha_{min}\mu^2 d_T s\right)g_{ec}, \end{aligned} \quad (2)$$

$$g_{leaf,\,op} = \frac{D_{wa}\pi\alpha_{op}^2\mu^2 d_T s}{V_{ma}\left(4j+\pi\sqrt{\alpha_{op}}\right)(x'+\alpha_{op}\mu\sqrt{s})} + \left(2-\frac{\pi}{4}\alpha_{op}\mu^2 d_T s\right)g_{ec}. \quad (3)$$

$$g_{leaf,\,max} = \frac{D_{wa}\pi\mu^2 d_T s}{V_{ma}(4j+\pi)(x'+\mu\sqrt{s})} + \left(2-\frac{\pi}{4}\mu^2 d_T s\right)g_{ec}, \quad (4)$$

Equations (2) and (3) for $g_{leaf,min}$ and $g_{leaf,op}$, i.e. for leaves in which stomata are partially closed, have a key application: they enable the estimation of mean minimum and operational absolute or relative stomatal apertures, $a_{min}$ (or $\alpha_{min}$) and $a_{op}$ (or $\alpha_{op}$), respectively, by numerical inversion (i.e. adjusting aperture iteratively in Equation (2) or (3) until the observed value of $g_{leaf}$ is produced), given other known parameter values.

Furthermore, these equations can be analyzed for the causal influences of the inputs on the outputs. We first quantified the contributions of variation in each underlying parameter ($d$, $s$, $\alpha$, and $g_{ec}$) to variation in $g_{leaf}$ due to intrinsic sensitivity (intrinsic causality), all else being equal. To compute intrinsic sensitivities, we calculated $g_{leaf}$ first using the median values of $d$, $s$, $\alpha$, and $g_{ec}$ across species or genotypes, then reduced or increased those values by 10% individually, holding all else equal. Analyzing Equations (2)–(4) for $g_{leaf,min}$, $g_{leaf,op}$, and $g_{leaf,max}$ in this way (Supplementary Fig. S1) showed that all are sensitive intrinsically to small shifts in $d$ and $s$, but that $g_{leaf,op}$ and $g_{leaf,max}$ are insensitive to $g_{ec}$ [$g_{leaf,max}$ is insensitive to $\alpha$ because $\alpha$ is constant (=1) for $g_{leaf,max}$]. Notably, when comparing leaves within and across species, all variables differ simultaneously; thus, the intrinsic sensitivity of $g_{leaf}$ variation to each underlying factor does not determine their relative importance, which can be determined using realized causality analysis (see below).

## Variation across species and life forms in stomatal conductance, anatomy, and aperture

Our analysis of the compiled database showed a strong variation across species in $g_{leaf,min}$, $g_{leaf,op}$, and $g_{leaf,max}$, $d$, and $s$ (Fig. 2; Supplementary Tables S4 to S6). Using Equations (2) and (3), based on measurements of $g_{leaf,min}$, $g_{leaf,op}$, stomatal anatomy, and $g_{ec}$, we estimated stomatal apertures for all studied species, with stomatal aperture at minimum ($a_{min}$) or open for operational gas

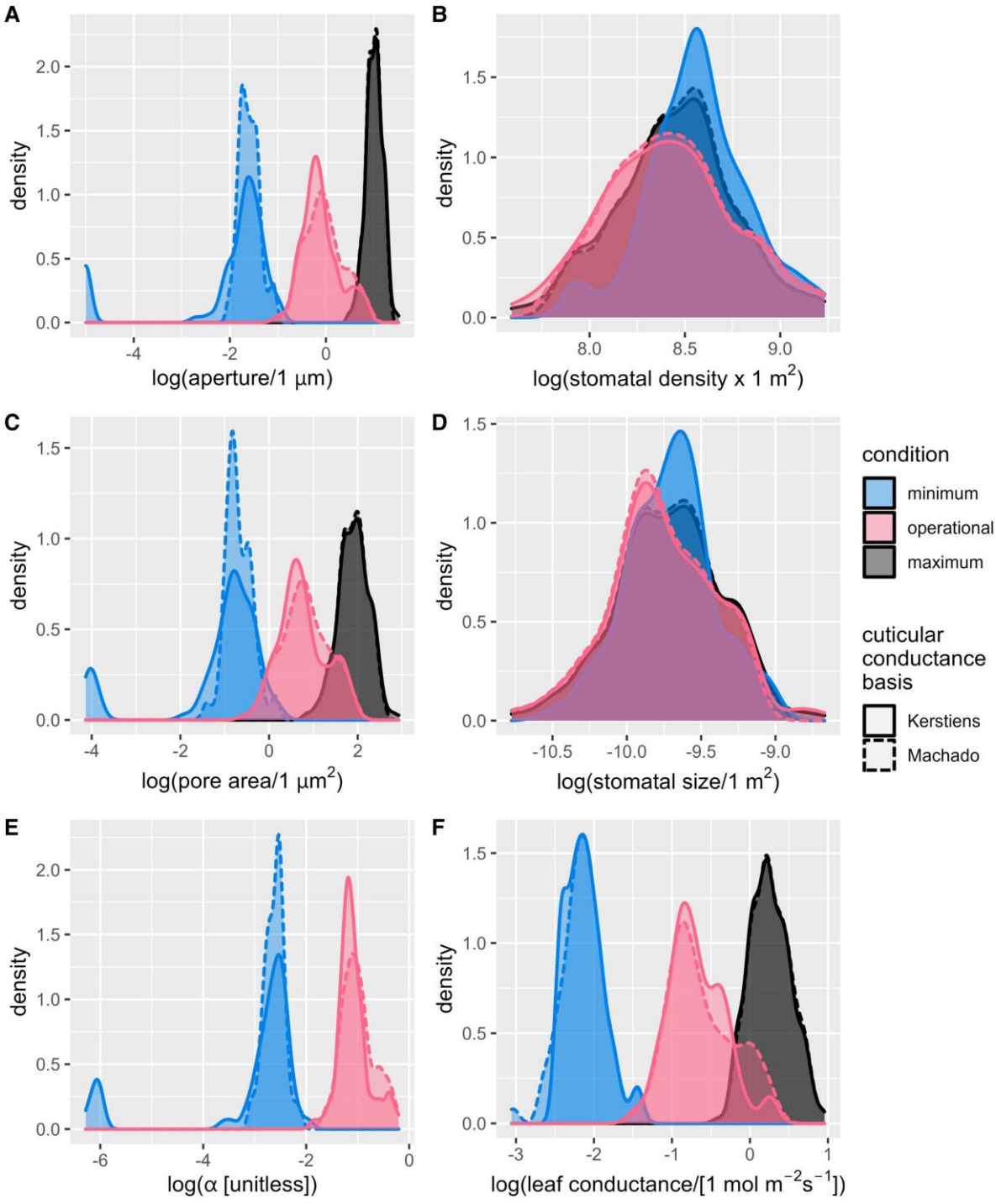


**Figure 2.** Distributions of variables in the database analyzed in this study. **A**) Stomatal aperture, $a$; **B**) stomatal density, $d$; **C**) pore area; **D**) stomatal size, $s$; **E**) fractional stomatal aperture, $\alpha$; and **F**) leaf surface conductance, $g_{leaf}$. Colors: blue, minimum leaf surface conductance ($g_{leaf,min}$); red, operational leaf surface conductance ($g_{leaf,op}$); and black, maximum leaf surface conductance ($g_{leaf,max}$). Line styles: solid, cuticular conductance estimated by bootstrapping from the distribution of values reported by Kerstiens (1996); dashed, cuticular conductance estimated from $g_{leaf,min}$ using correlation from Machado et al (2021). ("Maximum" is absent from panel **D** because $\alpha_{max} \equiv 1$).

exchange ($a_{op}$, i.e., as assessed for measurements of $g_{leaf,op}$ under ambient or saturating irradiance; see *Materials and methods*; Supplementary Table S1) or completely open to a circular pore ($a_{max}$; Fig. 2). Across all species in the database, $a_{min}$ ranged from $1.0 \times 10^{-11}$ m for common ivy (*Hedera helix*) to $1.1 \times 10^{-7}$ m for *Arabidopsis* (*Arabidopsis thaliana*) Col-0 ($2.6 \times 10^{-8}$ m average across all species/genotypes), $a_{op}$ ranged from $9.0 \times 10^{-8}$ 0.092 m for *Nothobaccaurea pulvinata* to $7.6 \times 10^{-6}$ m for *A. thaliana* genotype SPCH 2-4A ($1.1 \times 10^{-6}$ $\mu$m on average), and $a_{max}$ estimated from pore length ranged from $2.9 \times 10^{-6}$ m for white stopper (*Eugenia axillaris*) to $3.3 \times 10^{-5}$ m for royal fern (*Osmunda regalis*) ($1.1 \times 10^{-5}$ m on average). We note that $a_{max}$, the maximum pore aperture of a round pore, is a theoretical index that may never be achieved in vivo, especially in ferns, which do not open stomata by displacing the outer walls of the guard cells (Franks and Farquhar 2007). Considering apertures as fractions of their theoretical maximum,

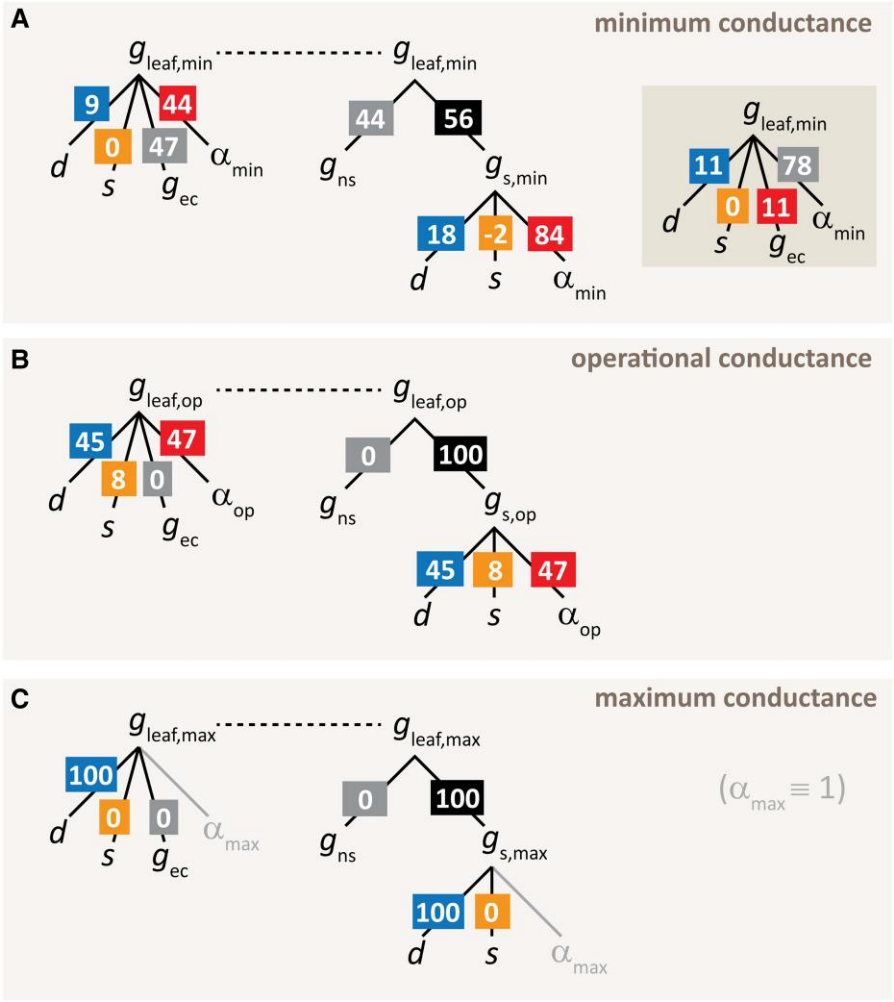


**Figure 3.** Realized causation of leaf surface conductance ($g_{leaf}$) by stomatal anatomy and behavior and epidermis + cuticular conductivity. Direct and hierarchical causal partitioning shown within each panel for the **A**) minimum, **B**) operational, and **C**) maximum leaf surface conductances ($g_{leaf,min}$, $g_{leaf,op}$, and $g_{leaf,max}$, respectively). Thus, on the left, $g_{leaf,min}$, $g_{leaf,op}$, and $g_{leaf,max}$ are partitioned as direct functions of stomatal density ($d$) and size (s), epidermis + cuticular conductivity ($g_{ec}$), and minimum, operational, and maximum fractional apertures ($\alpha_{min}$, $\alpha_{op}$, and $\alpha_{max}$, respectively). Additionally, on the right, $g_{leaf,min}$, $g_{leaf,op}$, and $g_{leaf,max}$ are partitioned hierarchically as functions of nonstomatal conductance ($g_{ns}$, closely related to $g_{ec}$) and minimum, operational, and maximum stomatal conductances ($g_{s,min}$, $g_{s,op}$, and $g_{s,max}$, respectively), in turn, as functions of $d$, s, and $\alpha_{min}$, $\alpha_{op}$, and $\alpha_{max}$, respectively. Values in colored boxes are % contributions of each parameter to differences in $g_{leaf}$ between species and genotypes (medians across all possible pairwise comparisons) for all studies combined. In **A**, the inset at the right gives the means of results from repeating all partitioning for $g_{leaf,min}$ for 150 times, each time randomly sampling a value of cuticular conductance for each species/genotype from the distribution of values in Kerstiens (1996). The corresponding standard errors are 0.1 ($d$), 0.1 ($s$), 0.5 ($g_{ns}$), and 0.4 ($\alpha$).

$\alpha_{min}$ ranged from $5.2 \times 10^{-7}$ for Indian hawthorn (*Rhaphiolepis indica*) to 0.011 for *A. thaliana* Col-0 (0.0024 on average) and $\alpha_{op}$ from 0.013 for *N. pulvinata* to 0.62 for *A. thaliana* genotype SPCH 2-4A (0.098 on average). $\alpha_{max}$ did not vary because it equals unity by definition. Our tests of the error in the estimation of $\alpha_{min}$ and $\alpha_{op}$ using this analytical approach showed lower coefficients of variation for these derived variables relative to those of the input measured variables in Equations (2) and (3) (i.e. $g_{leaf,min}$ or $g_{leaf,op}$, s, $d$, and $g_{ec}$; see Supplementary Method S3; Supplementary Table S7; Supplementary Fig. S2).

We compared the values for stomatal apertures estimated in our database using Equations (2) and (3) with those measured for 10 species in the literature (using top-view images from light, laser confocal, or scanning electron microscopy) for closed stomata in leaves dehydrated and/or in the dark, or exposed to ozone stress, relative to open stomata in control leaves (Supplementary Tables S8 and S9). When measured in images, the stomatal aperture values ranged up to orders of magnitude larger, whether considered in absolute terms or as a fraction of maximum (i.e. for both $a_{min}$ and $\alpha_{min}$), which ranged from 0 to 4.9 μm (1.62 μm on average) and 0 to 0.240 (0.070 on average), respectively. The lower values estimated using Equations (2) and (3) are consistent with the functional aperture of closed stomata being much smaller than that observed in the top view, given that the guard cell pore flares away from the inner pore (Fig. 1E; Franks et al. 1998).

## Causal partitioning of $g_{leaf,max}$, $g_{leaf,op}$, and $g_{leaf,min}$ with respect to stomatal traits

The causal partitioning of $g_{leaf}$ resolved the mechanistic roles of stomatal anatomy and behavior and $g_{ec}$ in determining variation within and across species, beyond the correlational patterns, which are influenced by covariation among variables (Figs. 3 and 4). Across all species in the database, on average, $g_{leaf,min}$ was causally codetermined by $g_{ec}$ and $\alpha_{min}$ by 47% and 44%, respectively, with 9% determination by $d$ and a negligible role for $s$ (Fig. 3A;

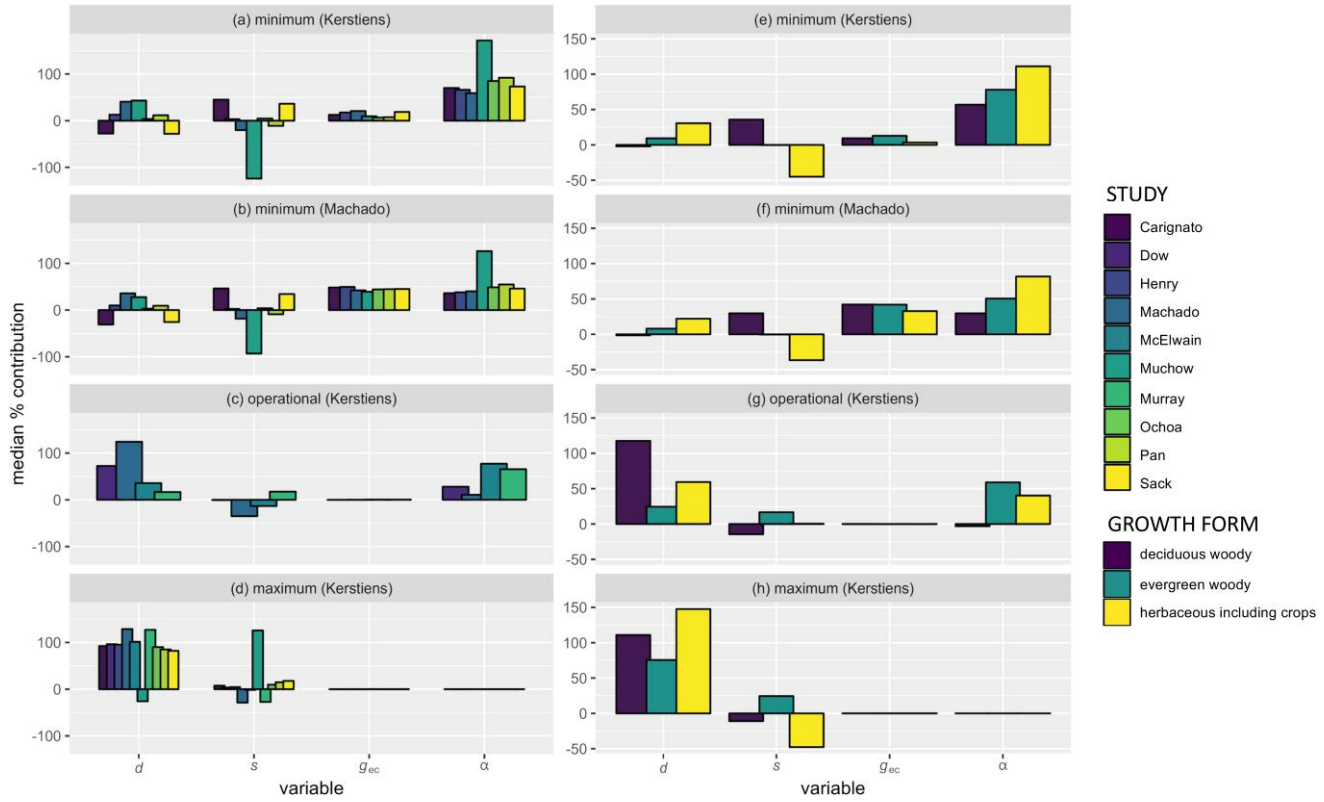


**Figure 4.** Results of causal partitioning of leaf surface conductance ($g_{leaf}$) by individual studies and growth form. $g_{leaf}$ was partitioned as a direct function of stomatal density ($d$) and size ($s$), epidermis + cuticular conductivity ($g_{ec}$), and fractional aperture relative to maximum ($\alpha$). The y-axis values are median % contributions of each factor to variation in minimum (panels **A**, **B**, **E**, and **F**: $g_{leaf,min}$), operational (panels **C** and **G**: $g_{leaf,op}$), and maximum (panels **D** and **H**: $g_{leaf,max}$) leaf surface conductance across all possible pairwise comparisons between species or genotypes within each study or growth form. Bars in panels **A**–**D** represent individual studies depicted in different colors: *Eucalyptus* genotypes (Carignato et al. 2019; $n = 9$); genotypes of *A. thaliana* (Dow et al. 2014; $n = 8$); California woody species (Henry et al. 2019; $n = 13$); Brazilian Cerrado species (Machado et al. 2021; $n = 30$); Cretaceous extant species (McElwain et al. 2016; $n = 18$); *S. bicolor* genotypes (Muchow and Sinclair 1989; $n = 10$); 75 diverse woody species (Murray et al. 2020; $n = 75$); California oak species (Ochoa, novel; $n = 15$); diverse woody species (Pan, novel; $n = 15$); and diverse tree and vine species (Sack et al. 2003a, 2003b; $n = 10$). Bars in panels **E**–**H** represent different growth forms depicted in different colors for angiosperms in the database (i.e. excluding the 1 fern and 4 gymnosperms from McElwain et al. 2016): evergreen woody, deciduous woody, and herbaceous, including crop species. For **A** and **E**, $g_{ec}$ was constrained by randomly sampling values of cuticular conductance for each species/genotype from the distribution of values given by Kerstiens (1996), repeating the entire procedure 150 times, and recording the mean of the results; and for panels **B**–**D** and **F**–**H**, $g_{ec}$ was inferred by estimating based on the regression against $g_{leaf,min}$ from the data of Machado et al. (2021).

Supplementary Table S10). For these analyses, $g_{ec}$ was estimated based on its regression against $g_{leaf,min}$ from Machado et al. (2021). We confirmed the finding that $g_{leaf,min}$ was only minimally influenced by $d$, and not by $s$, by estimating $g_{ec}$ instead by sampling values at random from the distribution of data given by Kerstiens (1996; Fig. 3A, inset). By contrast, on average, the $g_{leaf,op}$ was 47% determined by $\alpha_{op}$, 45% by $d$, and 8% by $s$ (Fig. 3B). Finally, $g_{leaf,max}$ was, on average, entirely determined by $d$ (Fig. 3C). Similar patterns were found in the causal partitioning analyses applied for the individual studies and for angiosperms of different life form groups (woody evergreen, woody deciduous, and herbaceous/crops; Fig. 4; Supplementary Table S10). Both within studies and within growth forms, $\alpha_{min}$ and $g_{ec}$ together were stronger causes of variation in $g_{leaf,min}$ than $d$ and $s$ considered together, $\alpha_{op}$ and $d$ were the dominant causes of $g_{leaf,op}$, and $d$ was by far the strongest cause of variation in $g_{leaf,max}$, with the exception of one study of genotypes of *S. bicolor* for which $s$ was the principal driver of variation in $g_{leaf,max}$ (Fig. 4).

## Testing the correlations of leaf surface conductances for diverse species across contexts

Across all growth forms, we found a weak association of $g_{leaf,min}$ with $g_{leaf,max}$ ($r = 0.27$, $P < 0.001$; Fig. 5A, purple line; Supplementary Table S11) and a weak relationship within deciduous woody species ($r = 0.20$, $P = 0.02$; Fig. 5A). A relationship was found within only 1/7 individual studies, that of tree species of Cerrado, a Brazilian savanna ($r = 0.48$; $P = 0.0076$; Supplementary Fig. S3; Machado et al. 2021). Much stronger relationships were found between $g_{leaf,op}$ and $g_{leaf,max}$ for each growth form considered separately and for all data pooled (Fig. 5B). There was a significant relationship between $g_{leaf,op}$ and $g_{leaf,max}$ for 3/4 studies ($r = 0.33$ to 0.96; $P < 0.001$; Supplementary Fig. S4; Supplementary Table S12) and for each of the 3 life form groups ($r = 0.47$ to 0.91; $P < 0.001$; Fig. 5B). The association across studies was represented by a fitted power law indicating a disproportionate increase in $g_{leaf,op}$ with increasing $g_{leaf,max}$ ($r = 0.63$; $P < 0.001$; Fig. 5B, purple line).

## Correlation of $g_{leaf}$, with stomatal size, density, and aperture, from minimum to minimum across individual and pooled studies

We tested the associations of $g_{leaf,min}$, $g_{leaf,op}$, and $g_{leaf,max}$ with stomatal anatomy ($d$ and $s$) and stomatal behavior, i.e., fractional stomatal opening ($\alpha$), across all species in the database and for individual studies and growth habits. Correlations of $g_{leaf,min}$ with $d$ and $s$ were found in a minority of individual studies and in certain life form groups, but not considering all species pooled. The

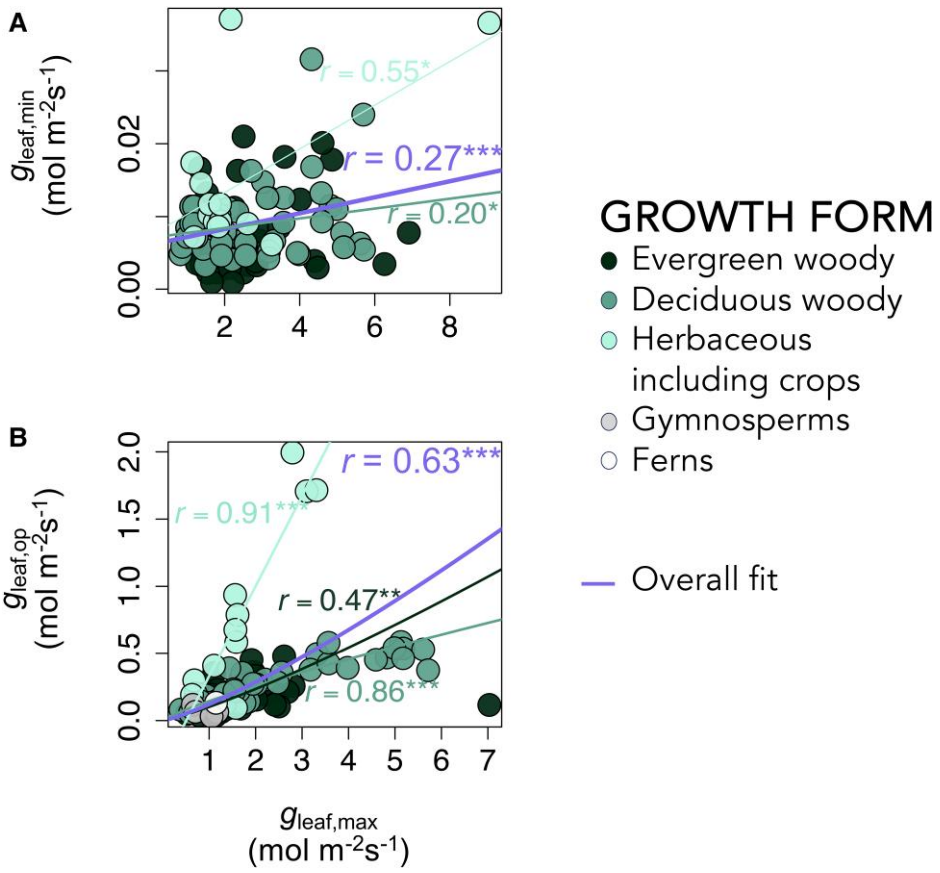


**Figure 5.** Testing relationships among leaf surface conductances with different states of stomatal opening across all species and within growth forms. Plots shown for the relationships of minimum **A**) and operational **B**) leaf surface conductance ($g_{leaf,min}$ and $g_{leaf,op}$, respectively) with maximum leaf surface conductance ($g_{leaf,max}$) across all species, and within growth forms (dark green, evergreen woody; green, deciduous woody; light green, herbaceous including crops) considered separately for angiosperms (i.e. excluding the 1 fern, white, and 4 gymnosperms, gray, from McElwain et al. 2016). In **A**, there is a significant linear relationship between $g_{leaf,min}$ and $g_{leaf,max}$ across all compiled species and genotypes ($n = 102$ for these traits; purple line) and within deciduous woody and herbaceous species ($n = 45$ and 13 for these traits, respectively; green and light green lines). In **B**, relationships were found for each growth form separately, with a linear relationship for herbaceous and crop species ($n = 12$) and power laws for evergreen woody species, deciduous species, and all species ($n = 63$, 44, and 133, respectively). $^{*}P \leq 0.05$; $^{**}P \leq 0.01$; $^{***}P \leq 0.001$.

$g_{leaf,min}$ was correlated with $d$ as described in the Introduction, for one study of 10 genotypes of *S. bicolor* (Muchow and Sinclair 1989) and one study of 30 species of Brazilian Cerrado (Machado et al. 2021), but not in the other 5 of 7 studies or considering data pooled across studies, although a positive association was found for herbaceous/crop species ($r = 0.74$; $P = 0.004$; Supplementary Fig. S5; Supplementary Table S13). These results were consistent with the causal partitioning analyses described above. Even in those two studies and for the herbaceous/crop species, $g_{leaf,min}$ depended on $d$ by only 22% to 36% (and only 8% on average across all the studies combined), and $g_{ec}$ and $\alpha_{min}$ drove the bulk of variation across species (Supplementary Table S9). Two of 7 studies showed a negative correlation of $g_{leaf,min}$ with stomatal size ($r = 0.39$ to 0.78; $P = 0.008$ to 0.031) and one showed a positive correlation ($r = 0.81$; $P = 0.0078$; Supplementary Fig. S6). The remaining 4 studies and pooled data across studies showed no correlation, and positive associations were found for deciduous woody and herbaceous species, including crops when considered separately ($r = 0.42$ to 0.52; $P = 0.002$ to 0.041; Supplementary Fig. S6). By contrast, $g_{leaf,min}$ was correlated with $\alpha_{min}$ as estimated using Equation (2) in 6/7 studies ($r = 0.75$ to 0.95; $P < 0.01$) for all growth forms when considered separately ($r = 0.56$ to 0.84; $P < 0.001$) and for studies' data pooled overall ($r = 0.75$; $P < 0.001$; Supplementary Fig. S7).

For $g_{leaf,op}$, correlations with stomatal density were stronger, with positive associations in 2/4 studies ($r = 0.42$ to 0.97; $P < 0.001$) for herbaceous/crop and deciduous woody species considered separately ($r = 0.28$ to 0.80; $P = 0.02$ to 0.001) and for studies' data pooled overall ($r = 0.42$; $P < 0.001$; Supplementary Fig. S8; Supplementary Table S14). Furthermore, $g_{leaf,op}$ was negatively associated with $s$ for one study ($r = -0.50$; $P = 0.003$) and for deciduous woody species ($r = -0.31$; $P = 0.03$), but not for data combined overall (Supplementary Fig. S9). Notably, $g_{leaf,op}$ was strongly related to $\alpha_{op}$ as estimated using Equation (3) for 3/4 studies ($r = 0.65$ to 0.85; $P < 0.01$), for herbaceous/crops and evergreen woody considered separately ($r = 0.67$ to 0.90; $P < 0.001$), and for all data combined ($r = 0.69$; $P < 0.001$; Supplementary Fig. S10). While $\alpha_{min}$ and $\alpha_{op}$ were estimated from $g_{leaf,min}$ and $g_{leaf,op}$, respectively, it is not a foregone conclusion that they would be correlated due to this determination, as the estimation of $\alpha_{min}$ and $\alpha_{op}$ also depended on $d$, $s$, and $g_{ec}$, as shown by Equations (2) and (3). Indeed, for 1/7 studies, $g_{leaf,min}$ was not associated with $\alpha_{min}$, and for 1/4 studies, $g_{leaf,op}$ was not associated with $\alpha_{op}$ (Supplementary Figs. S7 and S10; Supplementary Tables S15 and S16). Rather, this analysis indicates that the variation in $g_{leaf,min}$ and $g_{leaf,op}$ could not be explained by $d$, $s$, and $g_{ec}$ (and thus it was importantly explained by $\alpha_{min}$ and $\alpha_{op}$).

$g_{leaf,max}$ was strongly correlated with its determinant $d$ for 9/10 studies individually ($r = 0.72$ to 0.98; $P < 0.001$), for all 3 life form groups considered separately ($r = 0.73$ to 0.93; $P < 0.001$), and for all species combined ($r = 0.80$; $P < 0.001$; Supplementary Fig. S11;

Supplementary Table S15). By contrast, $g_{leaf,max}$ was negatively associated with $s$ for only one study ($r = -0.58$; $P < 0.001$), positively associated for one study ($r = 0.73$; $P = 0.016$) and across evergreen woody species ($r = 0.26$; $P = 0.$ 0.0075), but not for all species combined (Supplementary Fig. S12; Supplementary Table S15). Within the one study that quantified $g_{ec}$, $g_{leaf,min}$, $g_{leaf,op,}$ and $g_{leaf,max}$, all 3 versions of $g_{leaf}$ were related to $g_{ec}$ ($r = 0.41$ to 0.96; $P < 0.02$; Supplementary Fig. S13).

## Discussion

Our analyses provide insight into $g_{leaf}$ across the range of leaf hydration status, including the associations of $g_{leaf,min}$, $g_{leaf,op}$, and $g_{leaf,max}$ and their different underlying causal drivers. Across all the 203 species or genotypes in the database, $g_{leaf,min}$ was weakly related to $g_{leaf,max}$. Our estimation of stomatal aperture and our causal partitioning analyses indicated that this relationship did not arise due to a shared basis in stomatal traits. Instead, we find a mechanistically independent variation in $g_{leaf,min}$ and $g_{leaf,max}$ within and across ecologically differentiated life form groups. By contrast, across all species, $g_{leaf,op}$ was causally strongly related to $g_{leaf,max}$ due to their shared determination by stomatal density, $d$. Our results showed a switching of the influence of the stomatal anatomy on $g_{leaf}$ across the range of stomatal openings, from closure to maximum opening. Thus, across diverse species, $\alpha_{min}$ and $g_{ec}$ are the strong determinants of $g_{leaf,min}$, and stomatal density and size ($d$ and $s$, respectively) play a small or negligible role. By contrast, across diverse species, $d$ and $\alpha_{op}$ are co-determinants of $g_{leaf,op}$, with little influence of $s$ and $\alpha_{op}$, and $d$ is the major determinant of $g_{leaf,max}$.

These analyses thus resolved controversies described in the Introduction arising from the conflicting results of previous studies of individual species sets that focused on correlation analyses alone to infer the roles of $d$ and $s$ in determining $g_{leaf,min,}$ $g_{leaf,op}$, and $g_{leaf,max}$ (Muchow and Sinclair 1989; Sack et al. 2003a; Machado et al. 2021; Slot et al. 2021). Based on our compiled database, excluding a few trends observed in individual studies, the results of our causality analyses were broadly consistent with the overall patterns of correlations of the $g_{leaf,min}$, $g_{leaf,op}$, and $g_{leaf,max}$ with their underlying factors within the bulk of studies and across the pooled data. The independence of $g_{leaf,min}$ from $g_{leaf,max}$ in 6/7 individual studies and their weak relationship when pooling all species' data corresponded to their differentiated causal drivers. Thus, causally, on average, $g_{leaf,min}$ was determined by $g_{ec}$ and $\alpha_{min}$, and $g_{leaf,max}$ by $d$. Our analyses, therefore, did not support a proposed mechanistically constrained association between high $g_{leaf,max}$ and $g_{leaf,min}$, which would constrain the drought tolerance of species with high gas exchange capacity (Machado et al. 2021). The ability to achieve high $g_{leaf,max}$ does not constrain the ability to minimize water losses, explaining why drought tolerant species often have high $d$—which enables rapid gas exchange in periods when water is available, known as an "avoidance strategy"—without an intrinsic consequence for $g_{leaf,min}$, which can be minimized through low minimum $\alpha$ and $g_{ec}$ to enable water retention during drought. Notably, in our database, high-yielding crops tended to have high $g_{leaf,min}$ and high $g_{leaf,op}$ relative to other plants (Fig. 5), which would contribute to their relative drought sensitivity and high productivity, a finding to be confirmed in future studies of a wider range of species. Our causal analyses show that this pattern is not due to high $g_{leaf,min}$ and high $g_{leaf,op}$ both being related to the same causal factors, and, thus, does not represent a mechanistic association since $g_{leaf,min}$ is driven by $\alpha_{min}$ and $g_{ec}$, whereas $g_{leaf,max}$ is driven by $d$.

An association of $g_{leaf,min}$ and $g_{leaf,op}$ in specific plant groups would, thus, arise from a distinct selection of those traits due to ecology or breeding. Indeed, a high $g_{leaf,max}$ and $g_{leaf,op}$ would contribute to their high yield, whereas a high $g_{leaf,min}$ would be associated with less investment in the potentially costly cuticle and thick epidermal cell walls and perhaps with other potential functions and benefits hypothesized in the literature, but yet to be tested, such as nocturnal transpiration or foliar water uptake (Berry et al. 2019; Wang et al. 2021). These findings also indicate that species may be selected, and crop varieties bred, for both high productivity and minimal water loss during dehydrating conditions. Notably, additional stomatal traits may contribute to drought tolerance and/or high maximum gas exchange, as previous work on diverse species found a correlation between $g_{leaf,max}$ and sensitivity of stomatal conductance to dehydration (Henry et al. 2019) and that smaller stomata may respond more sensitively to dehydration and darkness (Aasamaa et al. 2001; Lawson and Blatt 2014).

Unlike for $g_{leaf,min}$, $d$ is a major determinant of $g_{leaf,op}$. Indeed, some studies suggested that $g_{leaf,op}$ can be well predicted from $g_{leaf,max}$, which implies that $d$ and $s$ would be the major determinants of $g_{leaf,op}$ across species (McElwain et al. 2016), although we found equal importance of $\alpha_{op}$ to $d$ and $s$ in causally determining variation across species in $g_{leaf,op}$. Notably, a low $g_{leaf,op}$ would tend to result in higher water use efficiency (WUE), as when stomatal conductance is reduced, WUE generally increases because reduced conductance leads to decreased intercellular $CO_2$ concentration— enhancing the $CO_2$ diffusion gradient—whereas the vapor gradient does not necessarily change (Farquhar and Sharkey 1982). Our findings suggest that differences across species in WUE, as for those in $g_{leaf,op}$, would be due to variation in both stomatal anatomy and fractional stomatal opening. Notably, we found a negligible influence of $g_{ec}$ on $g_{leaf,op}$ for the studies in our database, representing leaves under diurnal conditions under saturating irradiance. Recent studies, applying an approach to estimating $g_{ec}$ using gas exchange under varying irradiance qualities, estimated that $g_{ec}$ may play a larger role in determining $g_{leaf,op}$ when stomata are only slightly open under low irradiance or nocturnally (Márquez et al. 2022). These findings emphasize how the dynamics of stomatal behavior play a crucial role in the overall water and carbon management of plants and would influence their response to environmental stress and agricultural productivity.

For $g_{leaf,max}$, we found that, on average, $d$ is the causal determinant of variation across species, and that $s$, that is, a shorter pore distance in smaller stomata, is not generally a direct cause of average higher $g_{leaf,max}$ across species. Notably, $s$ and $d$ are generally negatively related in small species sets within and across plant lineages and over large, diverse species sets (Franks and Beerling 2009; Machado et al. 2021). Our analyses, based on causal partitioning, can disentangle the separate effects of $s$ and $d$ in driving a high $g_{leaf}$, resolving the key role of high $d$ rather than small $s$ as the causal driver of high $g_{leaf,max}$ (Figs. 3 and 4).

We derived a quantitative approach to estimating the relative stomatal aperture ($\alpha$) and its role in determining $g_{leaf,min}$ and $g_{leaf,op}$. The estimated apertures of closed stomata using our equations were far smaller than the measurements of published top-view micrograph images, a finding consistent with observations from the cross-sectional anatomy that the aperture of the stomatal throat can be far narrower than the apparently flared stomatal aperture visible in the top view (as illustrated in Fig. 1E). While the estimation of $\alpha$ contains uncertainty based on its derivation, we found this error to be less than those of the measurement

variables from which it is derived (Supplementary Table S7). We note that our estimate of $\alpha$ is an "effective" fractional aperture and the true value may be influenced by the second-order factors described in the Introduction, including deviations of the stomatal pore from simplified cylindrical geometry, the contribution of diffusion resistances in the intercellular airspaces, leaf surface features such as hairs or papillae surrounding the stomata, encryption of stomata, or stomatal clustering (Franks and Farquhar 2007; Roth-Nebelsick 2007; Kenzo et al. 2008; Hassiotou et al. 2009; Maricle et al. 2009; Feild et al. 2011; Lehmann and Or 2015). Future work is needed to analyze these effects, which were assumed to be relatively minor, based on the previous studies comparing $g_{leaf,op}$ and $g_{leaf,max}$ measurements with predictions based on anatomical determinants (Dow et al. 2014; McElwain et al. 2016; Murray et al. 2020; and this study, Fig. 5). Notably, the approach presented here to estimate $\alpha$ from Equations (2) and (3) for leaves with measured stomatal anatomy and measured or estimated $g_{ec}$ will enable the quantification of the responses of stomatal aperture for leaves under different environmental conditions (e.g. irradiance, VPD, or leaf dehydration). Similarly, Equations (2)–(4), which enable analyses of the responses of $g_{leaf}$ to stomatal anatomy, $\alpha$, and $g_{ec}$ across the full range of leaf hydration states, will enable future comparisons of the relative determinants of $g_{leaf}$ for different states of function across a wide range of contexts; for example, the influence of $\alpha_{min}$ versus $g_{ec}$ on $g_{leaf,min}$ or of $\alpha_{op}$ versus $d$ on $g_{leaf,op}$ across species in an evolutionary context or across crop varieties in breeding programs. Notably, models predicting survival during drought have emphasized $g_{leaf,min}$ as a major driver of leaf and plant survival during severe drought (Duursma et al. 2019; Billon et al. 2020; Cochard et al. 2021; Petek-Petrik et al. 2023) and proposed $g_{ec}$ and $d$ as its important determinants. Yet, our findings indicate a major role of $\alpha_{min}$, indicating that consideration of stomatal behavior is also critical in future modeling simulations of plant drought responses in crop and wild ecosystems.

Our causal partitioning analyses were robust across the data of studies individually and pooled. This congruity renders confidence in our conclusions, despite the uncertainty in our analysis due to the combination of data from multiple studies, and also the use of measured, derived, and inferred values for the components of stomatal conductance (Table 1). One limitation of our analysis, which provides avenues for future research, is our formulation of the maximum stomatal opening defined for stomata that open to a cylindrical pore (circular from the surface). Thus, $a_{max}$, $\alpha_{max}$, and $g_{leaf,max}$ are theoretical, given that pores would not open to these maxima under in vivo conditions. Like other theoretical physiological variables, such as photosynthetic parameters, including the maximum carboxylation rate ($V_{cmax}$), these maxima cannot be reached in practice but are useful for testing hypotheses regarding the capacity for stomatal diffusion and its drivers (Sack and Buckley 2016). Furthermore, this study focused almost entirely on angiosperms (Supplementary Table S3). In ferns, which have large stomata, the high maximum theoretical aperture, such as that estimated for *O. regalis*, may be much larger than that achieved in vivo, as when stomata open the guard cell walls are not displaced into the space occupied by surrounding epidermal pavement cells (Franks and Farquhar 2007; Cardoso et al. 2020, Westbrook and McAdam 2021). Future studies providing greater anatomical resolution of stomata open maximally for a greater diversity of species (cf. Franks and Farquhar 2007) may enable our approach to be extended to provide further clarity of the drivers of stomatal conductance. For example, with additional anatomical detail, the minimum fractional stomatal aperture relative to a circular pore, $\alpha_{min}$, may be further partitioned into its components i.e. as the product of the aperture relative to the *achievable maximum aperture* ($a_{min}/a_{max,achievable}$) and the achievable maximum aperture relative to the theoretical maximum of a circular pore ($a_{max,achievable}/a_{max}$).

Future work is also needed to better resolve the mechanisms and potential dynamics of $g_{ec}$. Previous work determining $g_{leaf,min}$ from abaxially sealed leaves or isolated cuticles has not always been consistent (Kerstiens 1996; Machado et al. 2021; Slot et al. 2021), and new methods based on gas exchange under different light qualities are promising. The potential shifts in $g_{ec}$ arising during leaf development (McAdam and Brodribb 2015), seasonally, or with changes in relative humidity (Kerstiens 1996) or temperature (Slot et al. 2021) indicate that its influence on $g_{leaf,min}$ would be similarly dynamic. Our equations provide an approach to disentangle the dynamic role of $g_{ec}$ on $g_{leaf}$ under varying conditions.

## Materials and methods

### Measurements of $g_{leaf,min}$ and stomatal traits

We measured $g_{leaf,min}$ and stomatal traits for 15 native California *Quercus* species in the California Botanic Garden in Claremont, California (34.110738°N, 117.713913°W; 507 mm precipitation per year; BioClim), in 2019 (Supplementary Tables S2 and S3). For each species, leaves were sampled from fully exposed branches of mature trees. Branches were transported from the field to the laboratory in plastic bags with wet paper towels to maintain hydration where they were re-cut underwater, placed in buckets, and enclosed in plastic bags lined with wet paper towels to rehydrate overnight (Sack and Scoffoni 2012). $g_{leaf,min}$ was measured using repeated gravimetric measurements (Sack and Scoffoni 2011) for 2 leaves from each of 3 individuals, for a total of 6 mature leaves for each species. The petioles of the excised leaves were sealed with wax, fresh mass was recorded, and the initial leaf scans were taken prior to leaf dehydration for 4 h above a large box fan to ensure stomatal closure. The leaves were then repeatedly measured for mass every 30 min over an additional 4 h period. The final leaf areas were scanned and processed on ImageJ2 (v2.14.0/1.54f). To calculate $g_{leaf,min}$, the slope of the mass against time was determined, converted to moles, divided by the ratio of VPD to atmospheric pressure, and normalized by the average of the initial and final leaf areas. The VPD was calculated using the Arden–Buck equation from the temperature and relative humidity in the lab based on a weather station (HOBO micro station; H21002).

The stomatal trait measurements were obtained from microscopy images taken from nail varnish impressions of both leaf surfaces of leaves fixed and preserved in a formalin–acetic acid–alcohol solution (FAA). From the microscope images of the nail varnish peels, the stomatal density ($d$) and stomatal area ($s$) were measured, and the maximum theoretical stomatal conductance [$g_{leaf,max}$; Franks and Farquhar 2007; Sack and Buckley 2016)] was calculated.

### Compilation and analysis of data from published literature on stomatal conductance and anatomy

Data were compiled from previous studies that reported $g_{leaf,min}$, $g_{leaf,op}$, and/or $g_{leaf,max}$ and stomatal anatomy after extensive searches in the literature (Supplementary Tables S2 and S3). These included studies of two or more species or genotypes within a species, including ferns, gymnosperms, and angiosperms, from 68 plant families grown under natural conditions or in

cultivation, or potted plants in greenhouses or growth chambers (Supplementary Table S2). We compiled data from 6 studies that in addition to $d$ and $s$, reported $g_{leaf,min}$ ($n = 9$ to 30 species or genotypes of a species), 3 studies that reported $g_{leaf,op}$ ($n = 9$ to 75 species or genotypes of a species), 1 study that reported measured $g_{ec}$ ($n = 30$; Machado et al. 2021), and additional $g_{ec}$ from a published data compilation ($n = 88$; Kerstiens 1996; Supplementary Table S16). Measurement methods and conditions are summarized in Supplementary Table S2. In these studies, $g_{leaf,min}$ was determined using the gravimetric approach (as used in this study for *Quercus* species; see previous section; Muchow and Sinclair 1989; Sack et al. 2003a; Carignato et al. 2019; Henry et al. 2019); $g_{leaf,op}$ was determined using a photosynthesis system (Dow et al. 2014; McElwain et al. 2016; Machado et al. 2021) or porometer (Murray et al. 2020); in one study, with low $CO_2$ to achieve maximal aperture (Dow et al. 2014); and $g_{ec}$ was determined by measuring the conductance of abaxially sealed leaves (Kerstiens 1996; Machado et al. 2021). Overall, $g_{leaf,min}$, $g_{leaf,op}$, $s$, $d$ (and thus $g_{leaf,max}$), and $g_{ec}$ were compiled for 102, 101, 203, and 30 species or genotypes, respectively. We calculated $g_{leaf,max}$ for all species from Equation (4) (see Results). Growth form (evergreen, deciduous, or herbaceous/crop) was determined using a literature search unless reported in the original study. Data were extracted from tables or from figure plots using ImageJ2 (v2.14.0/1.54f). A few corrections were made in compiling the data (Supplementary Table S3). For the data of Carignato et al. (2019), as adaxial stomata were denoted as "absent or extremely scarce," these were considered as absent, and $g_{leaf,min}$ was calculated by dividing "cuticular transpiration" by the mole fraction VPD derived from the Arden–Buck equation based on the average temperature and relative humidity data provided (Supplementary Table S1). For the data of Muchow and Sinclair (1989) on the genotypes of *S. bicolor*, only abaxial stomatal density was provided, along with a statement that observations on one variety showed 10% to 15% lower values on the adaxial surface and that pore length was approximately similar on both surfaces. We thus estimated adaxial stomatal densities as 12.5% lower than abaxial values across varieties and the pore lengths as the same (Supplementary Table S3). For all studies, we calculated whole-leaf $s$ and $g_{leaf}$, where relevant, as the stomatal density-weighted average of the values at each surface (e.g. $s_{leaf} = [s_{abaxial} \times d_{abaxial} + s_{adaxial} \times d_{adaxial}]/[d_{abaxial} + d_{adaxial}]$).

## Estimating stomatal aperture from scanning electron micrographs

To determine whether stomatal aperture could be estimated from scanning electron micrograph images, we compiled studies with measurements and images of open and closed stomata for 10 species from 9 families in 8 studies (Supplementary Tables S8 and S9). Measurements were extracted from images and graphs for the guard cell, stomatal pore length, pore area, and aperture width ($a$, measured as the central line between the exposed guard cell inner walls) using ImageJ2. When necessary, the pore length was estimated as half guard cell length or as pore area divided by aperture. With these data, we were able to estimate minimum stomatal apertures ($a_{min}$) for closed stomata and $\alpha_{min}$ as $a_{min}$ divided by the pore length of open stomata.

## Deriving equations for $g_{leaf}$ as a function of its determinants

We derived an expression for $g_{leaf}$ (Equation (1)) as the sum of parallel contributions from vapor loss through open pores, outer surfaces of guard cells, and outer surfaces of epidermal cells and adapted that expression for minimum, operational, and maximum values of $g_{leaf}$ (Equations (2)–(4), respectively) (full derivations are given in Supplementary Method S2). These derivations used the equation of Brown and Escombe (1900) to compute the effective conductance through stomatal pores based on stomatal and pore dimensions and contained an "end correction" to account for diffusion shells. We assumed that all pores were identical and that all solid leaf surfaces had identical conductances. We also included a correction to account for Knudsen diffusion through nearly closed stomatal pores, i.e., the reduced effective diffusivity when the size of a channel through which diffusion occurs is similar in magnitude to the mean free path of the diffusing species (Froment et al. 2011).

To apply this expression for $g_{leaf}$ to the estimation of the fractional stomatal aperture ($\alpha$) under conditions of either minimum or operational conductance, we numerically inverted the equation to solve for $\alpha$, given published values of $g_{leaf}$, cuticular conductance, stomatal density, and stomatal size. Numerical inversion was achieved by using the function "optimizeR" to find the value of aperture that minimized the squared difference between reported and calculated $g_{leaf}$, with search bounds of 0.00001 and 1.0 μm (for minimum conductance) or 0.01 and 20 μm (for operational conductance).

To constrain the uncertainty of our estimates of $\alpha$, we ran simulations to determine the error in $\alpha$ that would arise due to errors in its inputs (Supplementary Method S3). Using the Machado et al. (2021) dataset for 30 species for which $g_{leaf,min}$, $g_{ec}$, $s$, and $d$ were available (Supplementary Table S4), we (1) added a random noise with a given CV to each input variable ($s$, $d$, $g_c$, $g_{leaf,min}$); (2) for each species, we numerically solved for stomatal aperture, then calculated $\alpha$ as $a/p$; (3) we repeated steps (1) and (2) 1,000 times; (4) we repeated steps (1) to (3) for three values of CV (5%, 15%, or 30%, typical of the measured data in our study of *Quercus* species; Supplementary Table S17); (5) we repeated steps (1) to (4) with $g_{leaf,op}$ rather than $g_{leaf,min}$ as an input variable; and (6) we computed the CV of the resulting $\alpha$ values (across the 1,000 reps) for each group [each CV value and each type of $g_{leaf}$ (min, op)].

## Statistics

All statistical analyses and plots were performed using R software (4.0.5) and tidyverse and ggplot2 packages available from the CRAN platform.

## Causal partitioning analysis for drivers of variation in $g_{leaf,min}$, $g_{leaf,op}$, and $g_{leaf,max}$

We quantified the contributions of variation in each underlying parameter ($d$, $s$, $\alpha$, and $g_{ec}$) to variation in $g_{leaf}$ using intrinsic sensitivity (i.e. intrinsic causality) and causal partitioning (realized causality) analysis (Buckley and Diaz-Espejo 2015; Rodriguez-Dominguez et al. 2016; John et al. 2017; Fletcher et al. 2022). One advantage of causal partitioning analysis over correlation analysis is that the specific influences of individual drivers on the variable in question can be quantified. Correlation analysis is not able to do this ("correlation does not imply causation"), when the individual drivers are themselves correlated. Indeed, in certain cases, a variable $y$ may be positively correlated with a variable $x$ with which it is, in fact, negatively causally related. An elaborate illustration of this was provided by John et al. (2017)—see Fig. 2 in that paper—in which the leaf mass per unit area (LMA) was decomposed into its anatomical determinants, and correlation and causal partitioning analyses showed highly contrasting results.

Thus, for example, the LMA was strongly correlated with the number of cell layers in the upper epidermis; however, that factor was negligible as a causal driver of the LMA using either a sensitivity analysis of the equation for the LMA as a function of its anatomy and composition or causal partitioning analysis considering the drivers of variation in the LMA among species pairs.

Intrinsic sensitivity analysis was used to estimate the relative influences of input traits on $g_{leaf}$, all else being equal. To compute intrinsic sensitivities, we calculated three values of $g_{leaf}$ by using the median values of $d$, $s$, $\alpha$, and $g_{ec}$ across species or genotypes and by reducing or increasing those values by 10%. We repeated this twice: once using values of $g_{ec}$ estimated from $g_{leaf,min}$ using the Machado correlation (described below) and once using values of $g_{ec}$ sampled at random from the Kerstiens distribution (also described below). Causal partitioning analysis (Buckley and Diaz-Espejo 2015; Rodriguez-Dominguez et al. 2016; John et al. 2017) was used to determine the actual drivers of $g_{leaf}$ variation across the dataset against the actual background of trait variation. Briefly, this technique partitions a finite difference in the value of a dependent variable ($y$) between two states (a "reference" state, $y_r$, and a "comparison" state, $y_c$) into contributions from each of the independent variables ($x_1$, $x_2$, …, $x_n$), on which $y$ is functionally dependent ($y = y(x_1, x_2, \ldots, x_n)$), by integrating the total differential of $y$ ($dy$) between the two states. $dy$ is a sum of contributions from each independent variable:

$$dy = \frac{\partial y}{\partial x_1}dx_1 + \frac{\partial y}{\partial x_2}dx_2 + \ldots + \frac{\partial y}{\partial x_n}dx_n. \quad (5)$$

Integrating $dy$ between the reference and comparison states expresses the finite difference in $y$ ($\delta y \equiv y_c - y_r$) as a sum of the finite contributions from each independent variable:

$$\begin{aligned}\delta y \equiv y_c - y_r &= \int_r^c dy = \int_r^c \frac{\partial y}{\partial x_1}dx_1 + \int_r^c \frac{\partial y}{\partial x_2}dx_2 + \ldots + \int_r^c \frac{\partial y}{\partial x_n}dx_n \\ &= \delta y|_{x_1} + \delta y|_{x_2} + \ldots + \delta y|_{x_n}.\end{aligned} \quad (6)$$

By multiplying both sides by 100 and dividing by $\delta y$, the finite contributions (e.g. $\delta y|_{x_1}$) can be expressed as percentages of the total, giving percent contributions of each variable ($C[x_1]$, $C[x_2]$, …, $C[x_n]$) that sum to 100%:

$$\begin{aligned}100 \cdot \frac{\delta y}{\delta y} &= 100 \cdot \frac{\delta y|_{x_1}}{\delta y} + 100 \cdot \frac{\delta y|_{x_2}}{\delta y} + \ldots + 100 \cdot \frac{\delta y|_{x_n}}{\delta y} \\ &= C[x_1] + C[x_2] + \ldots + C[x_n] = 100.\end{aligned} \quad (7)$$

To apply this procedure in practice, one divides the interval between the reference and comparison states into many small intervals (100 in this study) and estimates each partial derivative in Equation (6) numerically for each small interval by calculating the values of $y$ at each end of the interval while changing only one independent variable at a time; e.g. denoting the endpoints of a given interval by subscripts $i$ and $f$, $\partial y/\partial x_2$ would be estimated as $[y(x_{1f}, x_{2f}, x_{3i}, \ldots, x_{ni}) - y(x_{1i}, x_{2i}, x_{3i}, \ldots, x_{ni})]/[x_{2f} - x_{2i}]$. This is repeated for each independent variable in each interval, and the results are summed over intervals to give $C[x_1]$, etc.

The functional relationships ($y(x_1, \ldots)$) of interest here were the dependences of $g_{leaf}$ on the underlying variables ($d$, $s$, $g_{ec}$, and $\alpha$), as given by Equations (1)–(4), and the differences of interest were the differences in observed $g_{leaf}$ between species and genotypes in each study. We thus repeated the procedure described above for every possible pairwise comparison between data points, for all studies combined (for $N$ data points, this gives $N \cdot (N-1)/2$ pairwise comparisons) and computed the median value of each contribution among all pairwise comparisons. For each pairwise comparison, we partitioned $g_{leaf}$ in two ways: hierarchically (first partitioning $g_{leaf}$ into $g_{ns}$ and $g_s$, then partitioning $g_s$ into $d$, $s$, and $\alpha$) and directly (partitioning $g_{leaf}$ into $d$, $s$, $g_{ec}$, and $\alpha$; see Supplementary Method S4). This procedure was repeated for each version of $g_{leaf}$ ($g_{leaf,min}$, $g_{leaf,op}$, and $g_{leaf,max}$).

Notably, the % causal contribution of any given variable $x$ to $y$ can be positive or negative, and, by definition, they add up to 100%. A positive % causal contribution for a factor $x$ indicates that, on average, $y$ differed between genotypes in the direction that one would expect, given the direction in which $x$ differed and the sign of the partial derivative of $y$ with respect to $x$. For example, if $\partial y/\partial x$ were positive, then one would expect $y$ to be larger in genotypes with larger $x$ (all else being equal). If this prediction is borne out, then the contribution of $x$ to $y$ is positive. If, however, $y$ tends to be smaller when $x$ is larger, despite $\partial y/\partial x$ being positive, this indicates that the positive effect of $x$ on $y$ is generally overcome by the other causative factors that are correlated with $x$ (John et al. 2017; Fletcher et al. 2022). An example of this would be stomatal density ($d$) and size ($s$): $\partial g_{leaf}/\partial d$ and $\partial g_{leaf}/\partial s$ are both positive, but $d$ and $s$ are themselves strongly negatively correlated with each other. Thus, if two species differ in $s$, it is not necessarily the case that the one with a greater $s$ will have a greater $g_{leaf}$ as well. In fact, the opposite more often turns out to be the case, thus giving $s$ a negative causal contribution to variation in $g_{leaf}$.

We used two alternative assumptions to constrain $g_{ec}$: (1) estimating $g_{ec}$ from the reported values of $g_{leaf,min}$ based on the empirical relationship between $g_{ec}$ and $g_{leaf,min}$ from Machado et al. (2021) ($n = 30$) (viz. $g_{ec} = 0.441 \cdot g_{leaf,min} - 0.0588$; $n = 30$, $r^2 = 0.933$) and (2) estimating $g_{ec}$ by sampling a value for each species/genotype at random from the distribution of $g_{ec}$ values given by Kerstiens (1996) ($n = 88$) and repeating this procedure many times to bootstrap the resulting distributions of parameter contributions. In case (2), we first fitted a beta distribution to the Kerstiens $g_{ec}$ data using the function "fitdist" from the package *fitdistrplus* (see Supplementary Fig. S14 for a comparison of observed and fitted distributions). We then repeated the partitioning many times, each time sampling a random $g_{ec}$ for each species/genotype. For $g_{leaf,min}$, we performed 150 sampling repeats. For $g_{leaf,op}$ and $g_{leaf,max}$, we performed only 5 repeats because the results differed negligibly due to the very small contribution of $g_{ec}$. We report the mean of each contribution computed across these sampling repeats. In each case, the standard error of the mean contribution across sampling repeats was less than 0.15%. For $g_{leaf,op}$ and $g_{leaf,max}$, due to the negligible importance of $g_{ec}$, results differed trivially between the two methods of estimating $g_{ec}$ described above (e.g. median absolute difference in % contributions was 0.25% for $g_{leaf,op}$ and 0.02% for $g_{leaf,max}$). The results from method 2 are available in Supplementary Fig. S2. Note that the reported values of $g_{ec}$ in Machado and Kerstiens were, in most cases, actual values of nonstomatal conductance ($g_{ns}$), which are expressed relative to the total area of the leaf surface, including the area of any open stomatal pores. Strictly, the value of $g_{ec}$ that applies to Equations (1)–(4) is expressed relative to the area of the leaf surface *excluding* open stomatal pores (but including guard cell surfaces); however, in practice, these two values differ negligibly when stomata are approximately closed (as when $g_{leaf,min}$ is being estimated), and the resulting difference between $g_{ec}$ and $g_{ns}$ was <0.03% in all cases examined here. When applied to operational or maximum $g_{leaf}$, however, nonstomatal and cuticular conductances can differ substantially (as much as 7.6% in the $g_{leaf,max}$ data used here, although the mean difference was 1.5%). In such cases, the contributions of variation in $g_{ec}$ (or $g_{ns}$) to variations in $g_{leaf,op}$ or $g_{leaf,max}$ are negligible anyway; thus, the distinction between $g_{ns}$ and $g_{ec}$ remains trivial.

We conducted the causal partitioning of $g_{leaf}$ into its components for each study individually and across all studies in the database. We also conducted causal partitioning for the angiosperm species (i.e. not including the 1 fern and 4 gymnosperms from McElwain et al. 2016 in this analysis) with data grouped by growth form (evergreen woody, deciduous woody, herbaceous/crop) rather than by study.

Additionally, to compare the results of causal partitioning with simple correlations of $g_{leaf}$ with its components, we tested Pearson's correlations between $g_{leaf,min}$, $g_{leaf,op}$, and $g_{leaf,max}$ with its components $d$, $s$, $\alpha$, and $g_{ns}$ and the correlations between $g_{leaf,min}$ vs $g_{leaf,op}$, $g_{leaf,min}$ vs $g_{leaf,max}$, and $g_{leaf,op}$ vs $g_{leaf,max}$. To test for relationships between leaf traits among species, each variable pair was fitted using either linear regressions with the "lm" in the Stats package or power laws fitted for using the function "smatr." We calculated Pearson's correlations for untransformed and log-transformed data and Spearman correlations for ranked data to test for either approximately linear or nonlinear (i.e. approximate power law) relationships, respectively, using the package "corrfx." The higher correlation value is reported in the text. These analyses were applied to data for all species and for individual studies and individual angiosperm growth forms.

## Author contributions

M.E.O., T.N.B., and L.S. designed the research; M.E.O., C.H., G.J., C.M., R.P., C.S., T.N.B., and L.S. performed the research; TNB contributed new analytic and computational data; M.E.O., T.N.B., and L.S. analyzed the data; and M.E.O., T.N.B., and L.S. wrote the paper with input from all authors.

## Supplementary data

The following materials are available in the online version of this article.

**Supplementary Method S1.** Reanalyzing the differences between minimum leaf surface conductance and leaf nonstomatal conductance in Slot et al. (2021).

**Supplementary Method S2.** Deriving equations for leaf surface conductance ($g_{leaf}$) as a function of its determinants.

**Supplementary Method S3.** Constraining the error in the derivation of fractional stomatal aperture ($\alpha$) based on Equations (2) and (3).

**Supplementary Method S4.** Explanation for the contributions of nonstomatal conductance ($g_{ns}$) and epidermal plus cuticle conductance ($g_{ec}$) differing between the results of causal partitioning analysis based on direct vs hierarchical partitioning of minimum leaf surface conductance ($g_{leaf,min}$).

**Supplementary Figure S1.** Intrinsic sensitivities of leaf surface conductance ($g_{leaf}$) to underlying parameters (% change in $g_{leaf}$ when a given parameter (as indicated on the left axis) shifts by 10%.

**Supplementary Figure S2.** Constraining the error of estimated minimum and operational fractional stomatal aperture ($\alpha$).

**Supplementary Figure S3.** Testing relationships between minimum and maximum leaf surface conductances ($g_{leaf,min}$ and $g_{leaf,max}$, respectively).

**Supplementary Figure S4.** Testing relationships between operational and maximum leaf surface conductances ($g_{leaf,op}$ and $g_{leaf,max}$, respectively).

**Supplementary Figure S5.** Testing relationships between minimum leaf surface conductance ($g_{leaf,min}$) and stomatal density ($d$).

**Supplementary Figure S6.** Testing relationships between minimum leaf surface conductance ($g_{leaf,min}$) and stomatal size ($s$).

**Supplementary Figure S7.** Testing relationships between minimum leaf surface conductance ($g_{leaf,min}$) and minimum fractional aperture ($\alpha_{min}$).

**Supplementary Figure S8.** Testing relationships between operational leaf surface conductance ($g_{leaf,op}$) and stomatal density ($d$).

**Supplementary Figure S9.** Testing relationships between operational leaf surface conductance ($g_{leaf,op}$) and stomatal size ($s$).

**Supplementary Figure S10.** Testing relationships between operational leaf surface conductance ($g_{leaf,op}$) and operational fractional aperture ($\alpha_{op}$).

**Supplementary Figure S11.** Testing relationships between maximum leaf surface conductance ($g_{leaf,max}$) and stomatal density ($d$).

**Supplementary Figure S12.** Testing relationships between maximum leaf surface conductance ($g_{leaf,max}$) and stomatal size ($s$).

**Supplementary Figure S13.** Testing relationships of epidermal + cuticle conductance ($g_{ec}$) with minimum, operational, and maximum leaf surface conductances ($g_{leaf,min}$, $g_{leaf,op}$, and $g_{leaf,max}$, respectively).

**Supplementary Figure S14.** Comparison of observed and fitted distributions of cuticular conductance.

**Supplementary Table S1.** Re-analysis of the data of Slot et al. (2021), Supplementary Fig. S1.

**Supplementary Table S2.** Published studies and novel data compiled for minimum leaf surface ($g_{leaf,min}$), operational leaf surface ($g_{leaf,op}$), and maximum leaf surface ($g_{leaf,max}$) conductances with stomatal anatomical traits and growing conditions and locations.

**Supplementary Table S3.** Data compiled from published and novel studies of stomatal traits and minimum leaf surface conductance.

**Supplementary Table S4.** Data used in causal partitioning analysis of minimum leaf surface conductance ($g_{leaf,min}$; one-sided leaf area basis) based on compiled data in **Supplementary Table S3**.

**Supplementary Table S5.** Data used in causal partitioning analysis of operational leaf surface conductance ($g_{leaf,op}$; one-sided leaf area basis) based on compiled data in **Supplementary Table S3**.

**Supplementary Table S6.** Data used in causal partitioning analysis of maximum leaf surface conductance ($g_{leaf,max}$; one-sided leaf area basis) based on compiled data in **Supplementary Table S3**.

**Supplementary Table S7.** Constraining the error of the estimation of fractional stomatal aperture ($\alpha$).

**Supplementary Table S8.** Compiled published studies with microscopic images in the top view of closed stomata with growing conditions and locations.

**Supplementary Table S9.** Estimates of stomatal aperture measured in microscopic images in the top view of closed and open stomata for 10 species from previously published studies described in **Supplementary Table S8**. Symbols and units defined in the legend below the data rows.

**Supplementary Table S10.** Results of causal partitioning analysis: contributions of each parameter to the differences in leaf surface conductance ($g_{leaf}$) between species or genotypes.

**Supplementary Table S11.** Correlation matrix for all studies combined and individual studies for minimum and maximum leaf surface conductances ($g_{leaf,min}$ and $g_{leaf,max}$, respectively).

**Supplementary Table S12.** Correlation matrix for all studies combined and individual studies for operational and maximum leaf surface conductances ($g_{leaf,op}$ and $g_{leaf,max}$, respectively).

**Supplementary Table S13.** Correlation matrix for all studies combined and for individual studies of minimum leaf surface conductance ($g_{leaf,min}$) and stomatal anatomy.

**Supplementary Table S14.** Correlation matrix for all studies combined and for individual studies of operational leaf surface conductance ($g_{leaf,op}$) and stomatal anatomy.

**Supplementary Table S15.** Correlation matrix for all studies combined and for individual studies of maximum leaf surface conductance ($g_{leaf,max}$) and stomatal anatomy.

**Supplementary Table S16.** Values of epidermal plus cuticular conductance ($g_{ec}$) reported by Kerstiens (1996).

**Supplementary Table S17.** Individual oak data for 15 native California oak species.

## Funding

This research was supported by the National Science Foundation grants 017949, 1951244, 1943583, 2307341, and 1557906 and the USDA NIFA Hatch Project 1016439.

*Conflict of interest statement.* None declared.

## Data availability statement

The data underlying this article are available in the article and in its online supplementary material.

## References

Aasamaa K, Sõber A, Rahi M. Leaf anatomical characteristics associated with shoot hydraulic conductance, stomatal conductance and stomatal sensitivity to changes of leaf water status in temperate deciduous trees. *Funct Plant Biol*. 2001:28(8):765–774. https://doi.org/10.1071/PP00157

Bauer H, Ache P, Lautner S, Fromm J, Hartung W, Al-Rasheid KAS, Sonnewald S, Sonnewald U, Kneitz S, Lachmann N, *et al*. The stomatal response to reduced relative humidity requires guard cell-autonomous ABA synthesis. *Curr Biol*. 2013:23(1):53–57. https://doi.org/10.1016/j.cub.2012.11.022

Berry ZC, Emery NC, Gotsch SG, Goldsmith GR. Foliar water uptake: processes, pathways, and integration into plant water budgets. *Plant Cell Environ*. 2019:42(2):410–423. https://doi.org/10.1111/pce.13439

Billon LM, Blackman CJ, Cochard H, Badel E, Hitmi A, Cartailler J, Torres-Ruiz JM. *The DroughtBox: a new tool for phenotyping residual branch conductance and its temperature dependence during drought (vol. 43, No. 6, pp. 1584–1594)*. Chichester, UK: John Wiley & Sons, Ltd; 2020.

Blackman CJ, Li X, Choat B, Rymer PD, Kauwe MGD, Duursma RA, Tissue DT, Medlyn BE. Desiccation time during drought is highly predictable across species of *Eucalyptus* from contrasting climates. *New Phytol*. 2019:224(2):632–643. https://doi.org/10.1111/nph.16042

Brown HT, Escombe F. Static diffusion of gases and liquids in relation to the assimilation of carbon and translocation in plants. *Proc R Soc Lond*. 1900:67:124–128. https://doi.org/10.1098/rstb.1900.0014

Buckley TN, Diaz-Espejo A. Partitioning changes in photosynthetic rate into contributions from different variables. *Plant Cell Environ*. 2015:38(6):1200–1211. https://doi.org/10.1111/pce.12459

Cardoso AA, Batz TA, McAdam SA. Xylem embolism resistance determines leaf mortality during drought in *Persea americana*. *Plant Physiol*. 2020:182(1):547–554. https://doi.org/10.1104/pp.19.00585

Carignato A, Vázquez-Piqué J, Tapias R, Ruiz F, Fernández M. Variability and plasticity in cuticular transpiration and leaf permeability allow differentiation of eucalyptus clones at an early age. *Forests*. 2019:11(1):9. https://doi.org/10.3390/f11010009

Cernusak LA, De Kauwe MG. Red light shines a path forward on leaf minimum conductance comment. *New Phytol*. 2022:233(1):5–7. https://doi.org/10.1111/nph.17794

Cochard H, Pimont F, Ruffault J, Martin-StPaul N. SurEau: a mechanistic model of plant water relations under extreme drought. *Ann For Sci*. 2021:78(2):1–23. https://doi.org/10.1007/s13595-021-01067-y

Diarte C, de Souza A X, Staiger S, Deininger A-C, Bueno A, Burghardt M, Graell J, Riederer M, Lara I, Leide J. Compositional, structural and functional cuticle analysis of *Prunus laurocerasus* L. Sheds light on cuticular barrier plasticity. *Plant Physiol Biochem*. 2021:158:434–445. https://doi.org/10.1016/j.plaphy.2020.11.028

Dow GJ, Bergmann DC, Berry JA. An integrated model of stomatal development and leaf physiology. *New Phytol*. 2014:201(4):1218–1226. https://doi.org/10.1111/nph.12608

Drake PL, Froend RH, Franks PJ. Smaller, faster stomata: scaling of stomatal size, rate of response, and stomatal conductance. *J Exp Bot*. 2013:64(2):495–505. https://doi.org/10.1093/jxb/ers347

Duursma RA, Blackman CJ, Lopéz R, Martin-StPaul NK, Cochard H, Medlyn BE. On the minimum leaf conductance: its role in models of plant water use, and ecological and environmental controls. *New Phytol*. 2019:221(2):693–705. https://doi.org/10.1111/nph.15395

Engineer C, Hashimoto-Sugimoto M, Negi J, Israelsson-Nordstrom M, Azoulay-Shemer T, Rappel W-J, Iba K, Schroeder J. $CO_2$ sensing and $CO_2$ regulation of stomatal conductance: advances and open questions. *Trends Plant Sci*. 2016:21(1):16–30. https://doi.org/10.1016/j.tplants.2015.08.014

Farquhar GD, Sharkey TD. Stomatal conductance and photosynthesis. *Annu Rev Plant Physiol*. 1982:33(1):317–345. https://doi.org/10.1146/annurev.pp.33.060182.001533

Feild TS, Jr UG, Chatelet DS, Brodribb TJ, Grubbs KC, Samain M-S, Wanke S. Fossil evidence for low gas exchange capacities for early cretaceous angiosperm leaves. *Paleobiology*. 2011:37(2):195–213. https://doi.org/10.1666/10015.1

Fernández V, Eichert T. Uptake of hydrophilic solutes through plant leaves: current state of knowledge and perspectives of foliar fertilization. *Crit Rev Plant Sci*. 2009:28(1–2):36–68. https://doi.org/10.1080/07352680902743069

Fletcher LR, Scoffoni C, Farrell C, Buckley TN, Pellegrini M, Sack L. Testing the association of relative growth rate and adaptation to climate across natural ecotypes of *Arabidopsis*. *New Phytol*. 2022:236(2):413–432. https://doi.org/10.1111/nph.18369

Franks PJ, Beerling DJ. Maximum leaf conductance driven by $CO_2$ effects on stomatal size and density over geologic time. *PNAS*. 2009:106(25):10343–10347. https://doi.org/10.1073/pnas.0904209106

Franks PJ, Cowan IR, Farquhar GD. A study of stomatal mechanics using the cell pressure probe. *Plant Cell Environ*. 1998:21(1):94–100. https://doi.org/10.1046/j.1365-3040.1998.00248.x

Franks PJ, Farquhar GD. The mechanical diversity of stomata and its significance in gas-exchange control. *Plant Physiol*. 2007:143(1):78–87. https://doi.org/10.1104/pp.106.089367

Froment GF, De Wilde J, Bischoff KB. *Chemical reactor analysis and design, 3rd ed*. Hoboken, N.J: Wiley; 2011.

Hassiotou F, Evans JR, Ludwig M, Veneklaas EJ. Stomatal crypts may facilitate diffusion of $CO_2$ to adaxial mesophyll cells in thick

sclerophylls. *Plant Cell Environ*. 2009:32(11):1596–1611. https://doi.org/10.1111/j.1365-3040.2009.02024.x

Henry C, John GP, Pan R, Bartlett MK, Fletcher LR, Scoffoni C, Sack L. A stomatal safety–efficiency trade-off constrains responses to leaf dehydration. *Nat Commun*. 2019:10(1):3398. https://doi.org/10.1038/s41467-019-11006-1

John GP, Henry C, Sack L. Leaf rehydration capacity: associations with other indices of drought tolerance and environment. *Plant Cell Environ*. 2018:41(11):2638–2653. https://doi.org/10.1111/pce.13390

John GP, Scoffoni C, Buckley TN, Villa R, Poorter H, Sack L. The anatomical and compositional basis of leaf mass per area. *Ecol Lett*. 2017:20(4):412–425. https://doi.org/10.1111/ele.12739

Kenzo T, Yoneda R, Azani MA, Majid NM. Changes in leaf water use after removal of leaf lower surface hairs on *Mallotus macrostachyus* (Euphorbiaceae) in a tropical secondary forest in Malaysia. *J For Res*. 2008:13(2):137–142. https://doi.org/10.1007/s10310-008-0062-z

Kerstiens G. Cuticular water permeability and its physiological significance. *J Exp Bot*. 1996:47(12):1813–1832. https://doi.org/10.1093/jxb/47.12.1813

Lawson T, Blatt MR. Stomatal size, speed, and responsiveness impact on photosynthesis and water use efficiency. *Plant Physiol*. 2014:164(4):1556–1570. https://doi.org/10.1104/pp.114.237107

Lehmann P, Or D. Effects of stomata clustering on leaf gas exchange. *New Phytol*. 2015:207(4):1015–1025. https://doi.org/10.1111/nph.13442

Liu C, Sack L, Li Y, Zhang J, Yu K, Zhang Q, Yu G. Relationships of stomatal morphology to the environment across plant communities. *Nat Commun*. 2023:14(1):6629. https://doi.org/10.1038/s41467-023-42136-2

López R, Cano FJ, Martin-StPaul NK, Cochard H, Choat B. Coordination of stem and leaf traits define different strategies to regulate water loss and tolerance ranges to aridity. *New Phytol*. 2021:230(2):497–509. https://doi.org/10.1111/nph.17185

Machado R, Loram-Lourenço L, Farnese FS, Alves RDFB, de Sousa LF, Silva FG, Filho SCV, Torres-Ruiz JM, Cochard H, Menezes-Silva PE. Where do leaf water leaks come from? Trade-offs underlying the variability in minimum conductance across tropical savanna species with contrasting growth strategies. *New Phytol*. 2021:229(3):1415–1430. https://doi.org/10.1111/nph.16941

Maricle BR, Koteyeva NK, Voznesenskaya EV, Thomasson JR, Edwards GE. Diversity in leaf anatomy, and stomatal distribution and conductance, between salt marsh and freshwater species in the C4 genus *Spartina* (Poaceae). *New Phytol*. 2009:184(1):216–233. https://doi.org/10.1111/j.1469-8137.2009.02903.x

Márquez DA, Stuart-Williams H, Farquhar GD. An improved theory for calculating leaf gas exchange more precisely accounting for small fluxes. *Nat Plants*. 2021:7(3):317–326. https://doi.org/10.1038/s41477-021-00861-w

Márquez DA, Stuart-Williams H, Farquhar GD, Busch FA. Cuticular conductance of adaxial and abaxial leaf surfaces and its relation to minimum leaf surface conductance. *New Phytol*. 2022:233(1):156–168. https://doi.org/10.1111/nph.17588

Martin-StPaul N, Delzon S, Cochard H. Plant resistance to drought depends on timely stomatal closure. *Ecol Lett*. 2017:20(11):1437–1447. https://doi.org/10.1111/ele.12851

McAdam SAM, Brodribb TJ. The evolution of mechanisms driving the stomatal response to vapor pressure deficit. *Plant Physiol*. 2015:167(3):833–843. https://doi.org/10.1104/pp.114.252940

McElwain JC, Yiotis C, Lawson T. Using modern plant trait relationships between observed and theoretical maximum stomatal conductance and vein density to examine patterns of plant macroevolution. *New Phytol*. 2016:209(1):94–103. https://doi.org/10.1111/nph.13579

Muchow RC, Sinclair TR. Epidermal conductance, stomatal density and stomatal size among genotypes of *Sorghum bicolor* (L.) Moench. *Plant Cell Environ*. 1989:12(4):425–431. https://doi.org/10.1111/j.1365-3040.1989.tb01958.x

Murray M, Soh WK, Yiotis C, Spicer RA, Lawson T, McElwain JC. Consistent relationship between field-measured stomatal conductance and theoretical maximum stomatal conductance in C3 woody angiosperms in four major biomes. *Int J Plant Sci*. 2020:181(1):142–154. https://doi.org/10.1086/706260

Petek-Petrik A, Petrík P, Lamarque LJ, Cochard H, Burlett R, Delzon S. Drought survival in conifer species is related to the time required to cross the stomatal safety margin. *J Exp Bot*. 2023:74(21):6847–6859. https://doi.org/10.1093/jxb/erad352

Rodriguez-Dominguez CM, Buckley TN, Egea G, de Cires A, Hernandez-Santana V, Martorell S, Diaz-Espejo A. Most stomatal closure in woody species under moderate drought can be explained by stomatal responses to leaf turgor. *Plant Cell Environ*. 2016:39(9):2014–2026. https://doi.org/10.1111/pce.12774

Roth-Nebelsick A. Computer-based studies of diffusion through stomata of different architecture. *Ann Bot*. 2007:100(1):23–32. https://doi.org/10.1093/aob/mcm075

Roussin-Léveillée C, Lajeunesse G, St-Amand M, Veerapen VP, Silva-Martins G, Nomura K, Brassard S, Bolaji A, He SY, Moffett P. Evolutionarily conserved bacterial effectors hijack abscisic acid signaling to induce an aqueous environment in the apoplast. *Cell Host & Microbe*. 2022:30(4):489–501.e4. https://doi.org/10.1016/j.chom.2022.02.006

Sack L, Buckley TN. The developmental basis of stomatal density and flux. *Plant Physiol*. 2016:171(4):2358–2363. https://doi.org/10.1104/pp.16.00476

Sack L, Cowan PD, Jaikumar N, Holbrook NM. The 'hydrology' of leaves: co-ordination of structure and function in temperate woody species. *Plant Cell Environ*. 2003a:26(8):1343–1356. https://doi.org/10.1046/j.0016-8025.2003.01058.x

Sack L, Grubb PJ, Marañón T. The functional morphology of juvenile plants tolerant of strong summer drought in shaded forest understories in southern Spain. *Plant Ecol*. 2003b:168(1):139–163. https://doi.org/10.1023/A:1024423820136

Sack L, Scoffoni C. Measurement of leaf hydraulic conductance and stomatal conductance and their responses to irradiance and dehydration using the evaporative flux method (EFM). *J Vis Exp*. 2012:4179. https://dx.doi.org/10.3791/4179

Sack L, Scoffoni C. Minimum epidermal conductance ($g_{min}$, a.k.a. cuticular conductance). *Prometheus: Protocols in Ecological & Environmental Science*. 2011. https://prometheusprotocols.net/function/gas-exchange-and-chlorophyll-fluorescence/stomatal-andnon-stomatal-conductance-and-transpiration/minimum-epidermal-conductance-gmin-a-k-a-cuticular-conductance/

Sack L, Tyree M. Leaf hydraulics and its implications in plant structure and function. In Holbrook NM, Zwieniecki MA (eds) *Vascular Transport in Plants*. Oxford, England: Elsevier, 93–114.

Slot M, Nardwattanawong T, Hernández GG, Bueno A, Riederer M, Winter K. Large differences in leaf cuticle conductance and its temperature response among 24 tropical tree species from across a rainfall gradient. *New Phytol*. 2021:232:1618–1631. https://doi.org/10.1111/nph.17626

Smith SE, Fendenheim DM, Halbrook K. Epidermal conductance as a component of dehydration avoidance in *Digitaria californica* and *Eragrostis lehmanniana*, two perennial desert grasses. *J Arid Environ*. 2006:64(2):238–250. https://doi.org/10.1016/j.jaridenv.2005.04.012

Wang Y, Anderegg WR, Venturas MD, Trugman AT, Yu K, Frankenberg C. Optimization theory explains nighttime stomatal

responses. *New Phytol.* 2021:230(4):1550–1561. https://doi.org/10.1111/nph.17267

Wang R, Yu G, He N, Wang Q, Zhao N, Xu Z, Ge J. Latitudinal variation of leaf stomatal traits from species to community level in forests: linkage with ecosystem productivity. *Sci Rep*. 2015:5(1):14454. https://doi.org/10.1038/srep14454

Westbrook AS, McAdam SA. Stomatal density and mechanics are critical for high productivity: insights from amphibious ferns. *New Phytol.* 2021:229(2):877–889. https://doi.org/10.1111/nph.16850

Wu L, de Boer HJ, Zixiao Z, Chen X, Shi Y, Peng S, Wang F. The coordinated increase in stomatal density and vein dimensions during genetic improvement in rice. *Agron J.* 2020:112(4):2791–2804. https://doi.org/10.1002/agj2.20180

Xie X, Wang Y, Williamson L, Holroyd GH, Tagliavia C, Murchie E, Theobald J, Knight MR, Davies WJ, Leyser HMO, *et al.* The identification of genes involved in the stomatal response to reduced atmospheric relative humidity. *Curr Biol*. 2006:16(9):882–887. doi:10.1016/j.cub.2006.03.028